# A Graph Theory Approach to Resilience of Transportation Infrastructure Systems: Accounting for Traffic Volume with Weighted Links

A Thesis

Presented to
the faculty of the School of Engineering and Applied Science
University of Virginia

in partial fulfillment
of the requirements for the degree

Master of Science

by

Elizabeth R. Engel

August

2016

APPROVAL SHEET

The thesis
is submitted in partial fulfillment of the requirements
for the degree of
Master of Science

Elizabeth R Engel
AUTHOR

The thesis has been read and approved by the examining committee:

Lindsay Ivey Burden, Ph.D.
Advisor

Brian Smith, Ph.D.

Jose Gomez, Ph.D., P.E.

Accepted for the School of Engineering and Applied Science:

James H. Aylor

Dean, School of Engineering and Applied Science

August
2016

## Abstract

A new paradigm for complex systems performance and maintenance decision-making is developing in the form of resilience engineering. Depending on the subject area, different definitions of resilience exist. In this project, we adopt a definition appropriate for resilience in transportation systems: the ability of the system to recover and adapt to external shocks, which include natural, intentional and technogenic disasters and failure due to poor design. These disturbances can ultimately affect the smooth and efficient operation of systems and may demand a shift of process, strategies and/or coordination.

This project builds off existing research and uses graph theory methods to develop a methodology to determine the resilience index of any transportation infrastructure system. This project also introduces weighting into the methodology based on traffic volume. Two weighting strategies are offered. It is shown that the inclusion of either weighting strategy increases the resilience of infrastructure systems and provides a more complete model. Finally, the methodology developed is applied to the network of major state and federal highways in Albemarle County, Virginia, to illustrate the process of determining a transportation infrastructure system's resilience index.

**Acknowledgments**

There are several people I would like to thank for their help, encouragement, and contributions toward the completion of my graduate studies at the University of Virginia:

First, I thank my advisor, Lindsay Ivey Burden. Lindsay welcomed me into her research group without ever meeting me face-to-face and gave me the opportunity to return to Virginia for my graduate work. For the past two years she has been kind and encouraging, even and especially when I encountered setbacks in my research. She always believed I could reach this point, even when my own belief faltered.

To the other members of my committee: Professor Brian Smith and Dr. Jose Gomez. Professor Smith, nothing I have accomplished in the past two years would have been possible without your leadership of our department. Dr. Gomez, I was lucky to have you as a professor during my time at UVA and I learned so much I hope to apply in my career. You are endlessly patient and supremely accommodating, and I thoroughly enjoyed the courses I took with you. Thank you both for serving on my committee.

Nii Attoh-Okine, Professor of Civil and Environmental Engineering at University of Delaware, thank you for your guidance and assistance on this research. Without your previous work studying infrastructure resilience this project would not exist. Thank you for bringing me into the project and sharing your knowledge with me.

I would like to thank the entire staff of the Civil and Environmental Engineering department at UVA, especially Peggy Gibson, Pat Gibson, and Jesse Johnson. Everyone has been so kind and helpful to me during my time here, and it’s always a pleasure to see smiling faces around the halls of Thornton. Thank you for all you do to ensure everything about our department runs smoothly.

Thank you to my friends and fellow graduate students who helped me with my research: to Julia Carroll for helping me navigate the National Bridge Inventory, and to Dan Plattenberger and Stuart Sheffield for assisting me with GIS tools. Thank you Colton, the TA of my programming class, without whom I would not have learned Matlab.

To my team, the friends who’ve helped me through my graduate school journey with their endless encouragement, support, and laughter: Sarah, Kassie, Katie, Erin, Ashley, Courtney, Lew, Ryan, Charles, and so many others who’ve been there for me from near and far. There’s not a better bunch out there and I am so lucky to have you.

Of course, thank you to my family for their love and support. To my parents, for raising me to be the person I am today and for encouraging me to follow my dreams, even though they’ve sometimes taken me far from home. To my mom, for copy editing this thesis and countless papers that came before it. To my dad, for pushing me to succeed and for never letting me forget how proud you are of me. And to my brother, for being my first friend and teaching me the things that only a brother can.

Finally, I’d like to thank the Mid-Atlantic Transportation Sustainability University Transportation Center (MATS UTC) for their financial support of this project.

## Table of Contents

**List of Figures**

## Introduction

Resilience engineering is developing as a new model for complex systems performance and maintenance decision-making.  People use engineered systems every day and rely on them to function as designed, even after a disturbance like a severe weather event or a terrorist attack.  The study of the ability of these systems, like a highway network or public transit mode, to function adequately after experiencing some external shock is the basis of the study of resilience.  Broadly, resilience is the ability of an entity to recover from or adjust easily to misfortune or change.  This definition is a helpful starting point when considering transportation infrastructure systems, but the complex and dynamic nature of these systems necessitates a more specific definition of resilience.  Resilience is a measure of the ability of a system to remain in a "safe envelope" under accident conditions, or its ability to safely and efficiently absorb changes of state variables while minimizing the duration and severity of any deviations from target performance levels [1, 2, 3].

The goal of this project is to develop a framework for measuring and quantifying the resilience of transportation infrastructure systems.  One widely used model is the R4 framework, developed by University of Buffalo's Multidisciplinary Center for Earthquake Engineering Research (MCEER).  In R4, resilience is broken down into four properties: robustness, redundancy, resourcefulness, and rapidity.  Robustness is the ability of systems and the elements that comprise them to withstand stress without loss of function, and redundancy is a measure of how many elements are substitutable in a system.  Resourcefulness is the capacity to identify issues and mobilize resources to solve them, while rapidity is a measure of the time the system and/or its elements require to recover from loss of function as a result of some stressor [4]. Most resilience engineering studies use the basis of R4 in their analysis and try to build on it in some useful way. This study is no different. In R4, each property is measured and reported separately. This study will develop a method to quantify all four properties of a system's resilience as a single value.

One way to represent resilience is graphically, using quality of infrastructure (QoI) curves and resilience triangles. Figure 1 plots a QoI curve for a system against time. The metric used to plot the QoI curve is case-dependent and can change based on what is important to the stakeholders for each system. For example, a good metric to use to represent QoI for an airport after an earthquake would be the percentage of flights coming in and going out compared to pre-earthquake numbers. A variety of other metrics could be gathered about the airport's infrastructure, such as the number of long-term parking spots available in the days and weeks following the earthquake. However, this information would not be as helpful in determining the overall resilience of the airport to the earthquake or to any other natural disasters or external shocks.

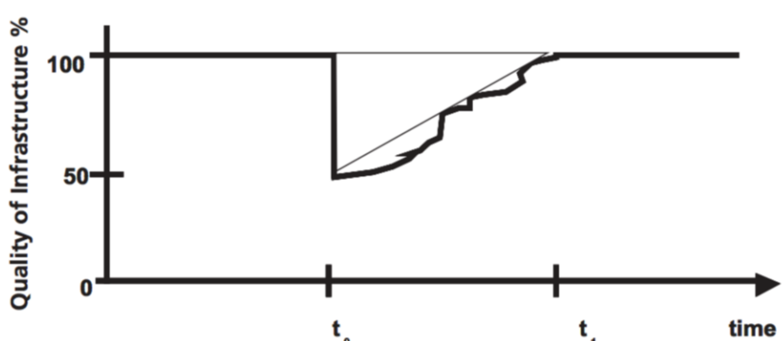


Figure 1. Resilience Triangle [5]

Plots like Figure 1 offer a straightforward view of what happens to a system's ability to perform at peak levels following some disaster or event. Before time $t_0$, the QoI curve is at 100%, indicating the system is functioning as designed. At $t_0$, some event occurs that drops the QoI curve to 50%. Between $t_0$ and $t_1$, the QoI curve gradually increases until the quality of infrastructure returns to 100%. This recovery will usually not be uniform or smooth, as shown in the figure. Resilience triangles are typically shown on the same plot as the QoI curve, as in Figure 1, and are a tool used to idealize the recovery of the system and quickly calculate resilience of the system.

Resilience triangles like that in Figure 1 can account for three of the four aspects of MCEER's R4 framework. Rapidity is measured by the time required to restore the system to full functionality, shown on the horizontal axis. Robustness and redundancy are both implicitly represented by the initial drop seen in QoI on the vertical axis. A smaller initial loss of functionality can signal information about the state of the system, but usually the magnitude of the initial loss correlates to at least one of the following three factors: the severity of the event itself, the robustness of the system, or the level of redundancy present in the system [5]. However, plots like Figure 1 are not the only representation needed when discussing resilience; there is a lot of information they do not provide, such as the costs associated with returning the system to full functionality or the resourcefulness of the entity examined. Adapting the plot to add a third dimension to account for resourcefulness, as shown in Figure 2, gives a more complete view of a system's resilience according to MCEER's R4 framework.

As more resources are mobilized after an event, the recovery time shortens. Theoretically, if enough resources were available, recovery time could be reduced until it was practically zero, but this is not possible in practice, due to necessary planning time before repairs can begin and different regulations in place depending on the location of the system [6].

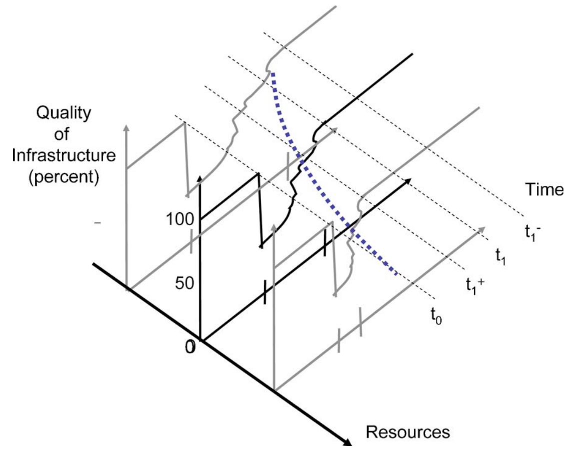

Figure 2: 3-D Resilience Triangle [6]

There are cases in which the quality of infrastructure curve never reaches 100% after an event. One example is New Orleans, Louisiana after it was devastated by Hurricane Katrina in August 2005. One year after the storm, the city's population was only 40% of what it was before Katrina hit; as of June 2015, almost a decade after the hurricane, population was 80% of what it had been pre-Katrina [7, 8]. The fact that population has still not reached the same levels as before the storm and that it has taken such a long time to achieve growth confirms what most already knew, that New Orleans' infrastructure before Hurricane Katrina was not very resilient.

On the other end of the spectrum, there are examples in which repairs necessitated by some external shock to an infrastructure system have increased the quality of that system over pre-event levels. One such case is the World Trade Center complex in lower Manhattan. After the terrorist attacks of September 11, 2001, all seven buildings in the complex were destroyed. The site is still being redeveloped, but once completed it will include 14.6 million square feet of floor space, an increase of more than 1 million square feet [9]. Additionally, site development includes the construction of an expanded transit hub that will provide more transportation links to the site than were available before 2001 [9].

**Motivation and Objectives**

Transportation infrastructure systems are some of the largest and most widely used engineered systems in the world; most people have a daily need to get from one place to another, and transportation networks are vital in the distribution of goods from production centers to points of consumption. While the quality of these infrastructure systems varies wildly, they have one thing in common: potential economic and productivity losses should a disaster occur. Disturbance in these systems also has the potential for massive loss of life.

In addition to this risk, transportation infrastructure is crucial to the movement of necessary consumer goods such as food and clothing from points of production to points of sale and consumption. This journey can often be quite long, crossing many state lines, regional borders or even entire oceans. Should there be a disruption in the transport of these goods, consumer wellbeing would suffer along with the economies of the producing and consuming nations.

While development of a resilience index could not prevent a disaster from occurring, it would be helpful in minimizing the effects of an external shock on a transportation infrastructure system and optimizing recovery and restoration efforts. A resilience index would help decision makers prioritize maintenance work and identify systems that should be retrofit. If systems that are not as resilient as we might like them to be can be identified, we can decrease the likelihood of injury or fatalities during catastrophic events and lessen the adverse economic effects, in addition to reducing recovery time.

Additionally, identifying the resilience indices of various infrastructure systems will increase disaster preparedness and enable better planning by emergency response and relief organizations. By having a more complete picture of how systems could be affected by various external shocks, planners can allocate more time and resources to more likely scenarios. Disaster planning also increases the ability of first responders to improvise in the field and adapt to the specific disaster scenario that might not have been predicted and explicitly planned for [7].

The purpose of this project is to develop and implement a framework for measuring the resilience of multimodal transportation infrastructure systems such as ports, highway systems, train stations, airports, etc. through development of a resilience index. Graph theory will be used to accomplish this goal, and the analysis will include weighting to account for traffic volume in the network. This project will consider natural and artificial external shocks as well as technogenic disasters through the implementation of different shock simulation strategies. The method will then be applied to the network of major state and federal highways in Albemarle County, Virginia.

## Literature Review

This section will summarize research that studies the resilience of highway systems. This summary highlights the myriad ways resilience of transportation infrastructure has been studied in the past and shows that there are many ways to analyze the same problem. This study uses graph theory to study resilience, and this section will also present an introduction to graph theory and define several terms that will be used throughout.  Then, this section presents a summary of how researchers have used graph theory and network science to evaluate transportation networks, identify their critical nodes and links, and determine their resilience.

*Highway Systems*

There are almost 250 million cars and trucks operating in the U.S. today, or almost one per person, and most will, at some point in their service life, be driven on an interstate highway [10]. The U.S. interstate highway system includes almost 50,000 miles of roadways, bridges, and tunnels and connects the country's big cities and small towns to one another.  The interstate highway system is vital for the movement of both people and goods across the country, and as such it is critical that it be resilient to external shocks.  Because it is so vast, it presents a unique challenge to those who wish to study its resilience.

In a report to Congress regarding seismic risk to highway infrastructure, it was established that a national database on seismic design and retrofit status of the highway system does not exist [11].  The Federal Highway Administration (FHWA) has developed software to estimate the loss of highway system capacity due to earthquakes, and this could possibly be used to model capacity loss for other shocks [11].  In the 20$^{th}$ century, the principal focus was on improving the resilience of highway structures such as bridges, and only recently has the focus turned to evaluating the system as a whole.  Even with this new focus on considering the whole system, bridges remain the most vulnerable piece of highway infrastructure, especially to seismic events [11].

One study defined the seismic resilience of highway bridges through the use of a loss function and a recovery function. The loss function includes direct and indirect losses suffered during restoration of a degraded system, and the recovery function models the quality of the infrastructure over time as the bridge is being restored. This research was applied to a California bridge that had suffered earthquake damage to its piers. The piers were retrofit with steel jackets, increasing their rotational ductility and decreasing the bridge's vulnerability to seismic events. Not only did the applied retrofit increase the seismic resilience of the bridge from 57.5% to 99.9%, the authors found that it was also cost effective. The financial benefits continued to increase with the service life of the bridge [12].

A study published in 2010 used data from two weather events (a blizzard in February 2008 and flooding in June 2008) to determine resiliency of an interstate corridor in Wisconsin. The approximately 290-mile stretch of I-90/94 runs southeast from Hudson, Wisconsin, on the border with Minnesota, through the state to its border with Illinois in Beloit, Wisconsin. The test corridor was described as a "critical backbone for freight and passenger mobility and accessibility in Wisconsin," as well as significant through traffic of passengers and freight between the Minneapolis and Chicago metropolitan areas and beyond [13]. The study used truck count and average truck speed through the different segments of the corridor as their quality of infrastructure (QoI) metrics to construct QoI curves and resilience triangles for the events. Figure 3 shows one of the curves constructed, using average truck speeds for the 40-mile segment between the small cities of Mauston and Portage in the days surrounding the February 2008 blizzard.

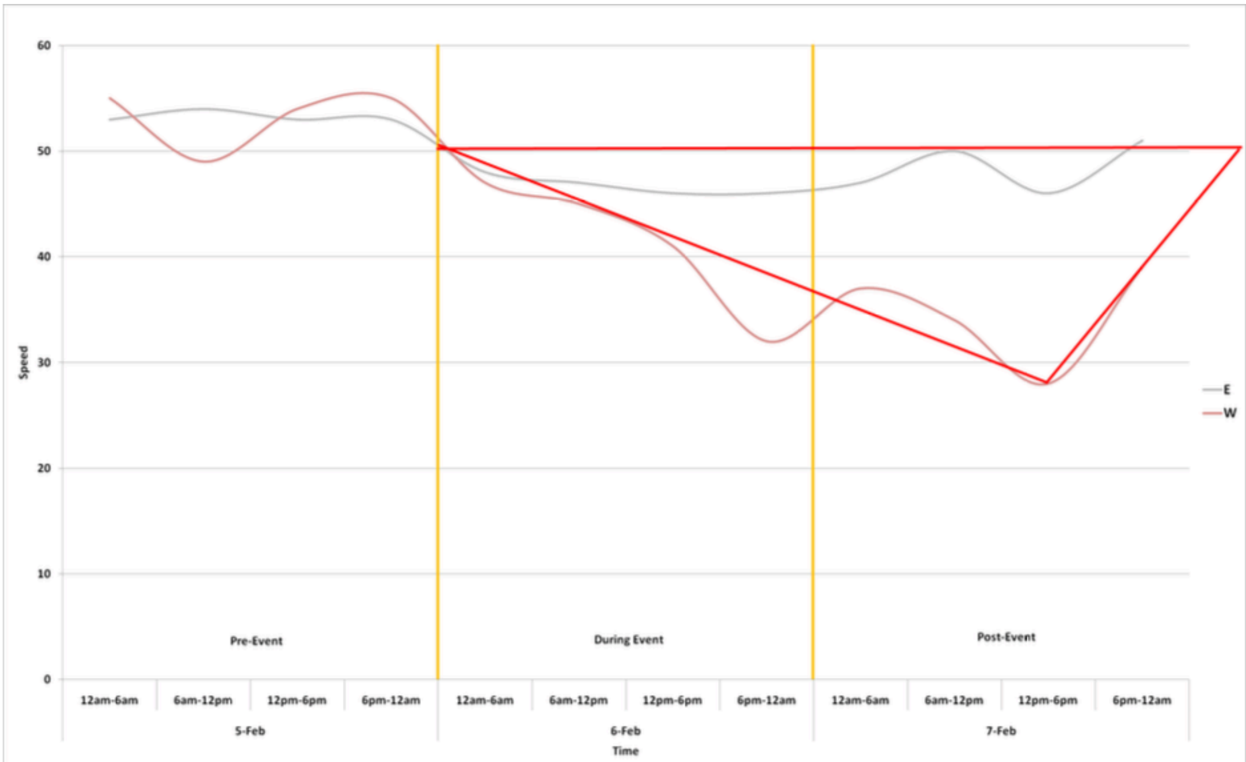

Figure 3: Speed resiliency on the Mauston to Portage section during the February 2008 event [13]

The authors of this study assert that two measures of the R4 framework can be measured from a plot such as the one in Figure 3: robustness and rapidity. Robustness is represented by the downward sloping section of the QoI curve, and rapidity by the section with positive slope. The authors fit resilience triangles to their data, seen in red in Figure 3, and then calculated the slopes and angles of the triangle's sides that corresponded to robustness and rapidity. They categorized their measures of robustness and rapidity as high, moderate or low depending on the measured angles. For robustness, measured by the downward sloping side of the resilience triangle, it's better to have a smaller angle, indicating a gentler or smaller decline in the QoI metric. However, for rapidity, larger angles are desirable because they indicate quicker recovery. The thresholds between the three categories are the same for robustness and rapidity, 11.3˚ and 26.6˚. For the case in Figure 3, the robustness angle is 21˚, indicating moderate robustness, and the rapidity angle is 51˚, indicating high rapidity. Different parts of the test corridor had distinct reactions to the two weather events. The more northern segments were affected less by both weather events. The blizzard had a bigger effect on the southern segment of the route, while a central segment was most heavily affected by flooding [13].

The studies discussed above, while useful in the study of transportation system resilience, offer only pieces of the puzzle that is the study of resilience. The results are case-specific and the metrics are often difficult to observe or calculate. The methods will need to be revised in order to apply them to other systems or systems subject to different disturbances. This study will fill the gaps left by these other studies by developing a method to determine the resilience index of any transportation infrastructure network subjected to any type of external shock.

*Graph Theory*

This project uses graph theory and network analysis to determine the resilience of a transportation infrastructure system. Graph theory and network science have been employed across various disciplines: in chemistry it has been used in drug design, and engineers have used it to evaluate complex infrastructure systems [14]. Recently, graph theory was even used to determine which characters hold the most power in the popular fantasy series “Game of Thrones” [15].

## Basics and Definitions

A network consists of a set of nodes – points representing a piece of infrastructure, such as a bridge or airport – and a set of links that connect them. A simple example network consisting of 4 nodes (n) and 4 links (m) is shown in Figure 4 below, and will be used to illustrate some of the pertinent terminology used in graph theory that will be used throughout this study.

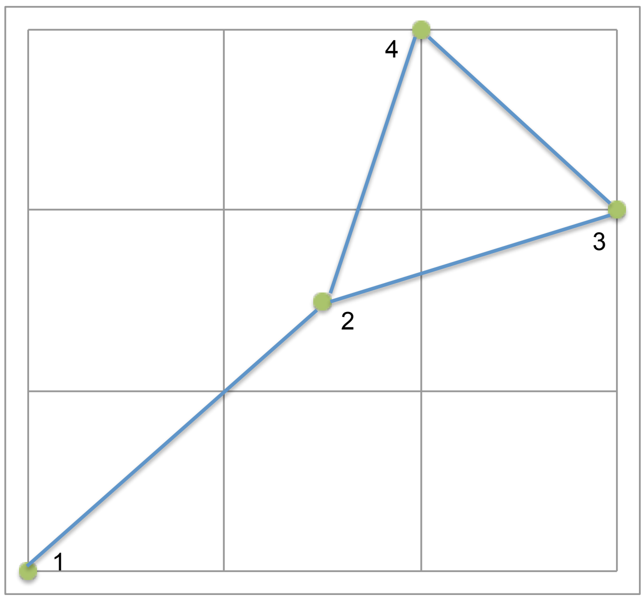

Figure 4: Simple Network

Links can be *directed* or *undirected*. A directed link allows travel in only one direction and is indicated with arrows, whereas an undirected link functions regardless of direction. All the links in this study are undirected.

A *path* between a pair of nodes exists if the nodes are connected by a link or several links passing through other nodes. If a path exists between every pair of nodes in the network, the network is *fully connected*. If not, it is *disconnected*. The simple network shown in Figure 4 is fully connected.

The *path distance* is the number of links in the path. Path distance can also be calculated using the length of each link in the path. In the network in Figure 4, there are two paths connecting nodes 1 and 4. The first path is 1-2-4, containing 2 links, and the second is 1-2-3-4, containing 3 links. The *shortest path* between nodes 1 and 4 is 1-2-4, and its path distance is 2.

The *diameter* of the network is the maximum value of the set of shortest paths between every pair of nodes in the network. The diameter of the simple network is 2.

Matrix methods are commonly used to represent and analyze networks. A network's *adjacency matrix, A*, is an n-by-n square matrix that represents linkages in a network. If a link exists between nodes *i* and *j*, the element *A(i,j)* is 1; if there is no link between the two nodes, the element is 0. Diagonal elements are always 0, and if the network has undirected links the matrix is symmetric. The adjacency matrix for the simple network is shown below.

$$A=\begin{bmatrix} 0 & 1 & 0 & 0 \\ 1 & 0 & 1 & 1 \\ 0 & 1 & 0 & 1 \\ 0 & 1 & 1 & 0 \end{bmatrix}$$

Various parameters are defined that describe the degree of connectedness of a network; these will be used to study the network's resilience. The parameters that will be used in this study are link density, average node degree, average shortest path distance, diameter, and betweenness centrality.

*Link density* is the relationship between the total number of links (m) in the network and the maximum number of links the network could support if every node (n) were connected to every other node by a single link. Link density is defined by Equation 1 below.

$$\text{Link Density} = \frac{2m}{n\,(n-1)} \qquad [16]\ (1)$$

Another important network property is *average node degree*. The *degree* of a node is how many links are connected to it. For a network with undirected links, average node degree can be calculated using Equation 2 below.

$$\text{Average Node Degree} = \frac{2m}{n} \qquad [16]\ (2)$$

The *average shortest path distance* for a network considers the shortest paths between every pair of nodes in the network, and can be calculated using equation 3 below.

$$\text{Average Shortest Path Distance} = \sum_{i\ j} \frac{l\,(i,j)}{n\,(n-1)} \qquad [16]\ (3)$$

where *l(i,j)* denotes the length of the shortest path between any two nodes *i* and *j*.

*Betweenness centrality* is an attribute of each node as opposed to one that describes the entire network. A node's betweenness centrality measures how often that node lies on the shortest path between other pairs of nodes in the network. A node need not have high degree or be centrally located in the network to have a high betweenness centrality. Betweenness centrality of a node is the ratio of the number of shortest paths between any pair of nodes (excluding the one in question) that pass through that node and the total number of shortest paths in the network (excluding those that begin and end at the node in question). The value of betweenness centrality is always between 0 and 1 and its formula is given in Equation 4 below.

$$\text{Betweenness Centrality of Node i} = \frac{1}{(n-1)(n-2)} \sum_{j,k \neq i} a_{jk(i)} \qquad [16]\ (4)$$

Where $a_{jk(i)}$ denotes if the shortest path between nodes *j* and *k* passes through node *i*. This value is 1 if the shortest path passes through node *i* and 0 if it does not.

The terms defined above are summarized in Table 1.

Table 1: Summary of Graph Theory Properties [16]

| Metric | Calculated for | Definition | Equation |
|---|---|---|---|
| Link Density | Network | The fraction between the total and the maximum number of links | $\frac{2m}{n\,(n-1)}$ |
| Average Node Degree | | The average value of the node-degree distribution | $\frac{2m}{n}$ |
| Average Shortest Path Distance | | Average value of the distances between all pairs of nodes | $\sum_{i\,j} \frac{l\,(i,j)}{n\,(n-1)}$ |
| Diameter | | Maximum shortest path distance between all pairs of nodes | $\max(\,L(i,j)\,)$ |
| Betweenness Centrality | Node | Proportion of shortest paths that run through a given node | $\frac{1}{(n-1)(n-2)} \sum_{j,k\neq i} a_{jk\,(i)}$ |

When using graph theory to study a network's resilience, the same basic method applies no matter the type of network. First, selected network properties are calculated. Then, nodes are removed from the system one at a time and the properties are recalculated. Two node removal strategies will be used in this study: a random node removal strategy (RNRS), and a targeted node removal strategy (TNRS). RNRS simulates disturbances to the system that have the same likelihood of occurring at any point in the system, like weather events or power outages. TNRS simulates deliberate attacks to important points in the network.

The first documented use of graph theory was by mathematician Leonhard Euler in 1741. He used what would become graph theory in his analysis of the problem known as "The Seven Bridges of Königsberg." The city of Königsberg, Prussia (modern day Kaliningrad, Russia) is divided into four separate landmasses by the Pregolya River. At the time, seven bridges connected the different landmasses (five of which still stand today). The layout of bridges and waterways is shown in Figure 5 below. The problem involved designing a walk through the city that involved crossing each bridge exactly once. It was not required that the walk begin and end in the same place. Many had tried to find a solution, but it was not until Euler modeled the problem as a graph, using the land masses as nodes and the bridges as links, that the it was shown it couldn't be done [17].

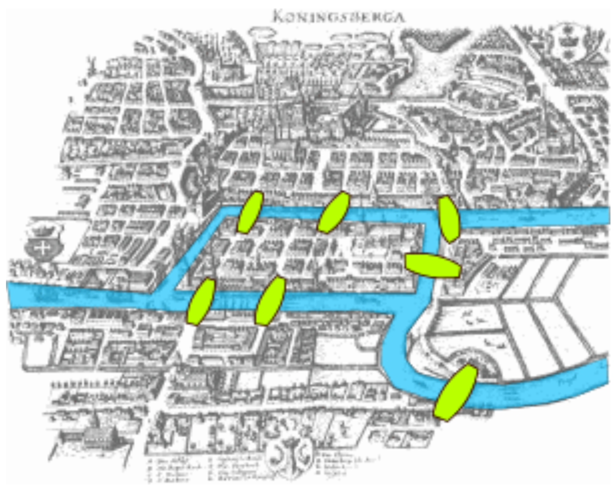

Figure 5: The Seven Bridges of Königsberg [18]

## Graph Theory in Resilience Engineering

Several studies have been performed using graph theory to study existing transportation networks. In a needs assessment report, Ham and Lockwood defined critical assets in the nation's highway transportation network as "those major facilities the loss of which would significantly reduce interregional mobility over an extended period and thereby damage the national economy and defense mobility" [19]. There are several topological network properties that can be used to identify these critical assets and aid in the prioritization of on-site evaluation and maintenance work. These topological properties rank the criticality and importance of the nodes and links in a network.

Ranking nodes by criticality and importance is the first step of implementing a targeted node removal strategy when using graph theory to study a network's resilience. The two topological properties most often used to determine the importance of nodes in a network are node degree and betweenness centrality. It's reasonable to assume that node degree and betweenness centrality are correlated for most networks and provide a good ranking of node importance. This is true for small networks, but the correlation breaks down as networks get larger [20]. Guimera and Amaral performed an analysis of the worldwide airport network that modeled airports as nodes and non-stop flights as links. Their results showed that the most central airports (represented by nodes with high degree) were not always the best connected to the rest of the network (nodes with high betweenness centrality). This is a reasonable result considering the size of their network: 3,883 nodes and over 27,000 links [21].

Reducing a network's functionality by removing the smallest possible amount of nodes is the goal of a targeted node removal strategy. Another study that used betweenness centrality to identify the most critical nodes recognized that by removing nodes with high betweenness, they disrupted the highest proportion of shortest paths in the graph. This affects movement through the graph and sends many paths on longer detours. This reduction in mobility is the very definition of a critical point in a graph [22].

In a study of the topological properties of the Italian airport network, betweenness centrality was used to locate the most important hubs in the network to prioritize maintenance at those locations [23]. Several studies found that when performing an analysis that includes targeted node removal to simulate deliberate attacks to a network, ranking the nodes based on betweenness centrality has a greater impact on topological properties than by ranking the nodes based on degree [20, 21]. Studies have also been done that remove nodes based on node degree, but these are less common than those that use betweenness centrality to rank nodes [Holmgren]. Betweenness centrality will be used in this study to determine node criticality for TNRS.

Employing a targeted node removal strategy to evaluate the network's response to disruption must also consider if the order of node removal will follow the initial node criticality ranking or if the ranking should be recalculated after each removal. A recalculated ranking after each node removal simulates a very sophisticated attack in which the perpetrators have knowledge of how the system will adapt to changes. In some cases, a node that originally had a very high degree or betweenness centrality could be isolated by the removal of one of its neighboring nodes, decreasing its degree or betweenness centrality and thus its importance to the network. Some studies only remove nodes based only on initial rankings but these might not be as useful as those studies that also use recalculated lists depending on the motivations and goals of the project [25].

In their research, Berche et. al analyzed the public transit networks of 14 cities around the world using 16 attack strategies. Half of these were based on removing nodes based on an initial node importance ranking and the other half used rankings that had been recalculated after each removal. They found that performing node removal based on recalculated importance ranking often led to steeper declines in the network's topological properties [26]. An analysis of a power supply and distribution also used initial and recalculated rankings and came to similar conclusions [24]. This study will use both initial and recalculated ranking to perform TNRS.

Others have developed different methods to determine which of a network's nodes are most critical. Ukkusuri and Yushimoto took a unique approach to determine which elements were most critical to a transportation network. They modeled the transit network in Manhattan during peak morning rush hour. Their network included bridges and tunnels that connect Manhattan to New Jersey and New York City's other boroughs, as well as the subway and bus systems within Manhattan itself. They chose to use average travel time as their metric for network performance. Travel time depends on the user's choice of route and travel mode, and user factors congestion into their decision-making process. Congestion is a function of the choices of all other network users [27].

The authors conducted their analysis using a network game with selfish players, each looking to optimize their own travel time with no regard for how their decisions affected other network users. With the original average travel time established, links were removed from the network one at a time, replacing the removed link before removing another one. The authors compared the average travel time data after they had removed each link in turn. They found that removing the bridges and tunnels into Manhattan had the greatest effect on average travel time. This result is not surprising, because they were modeling the network during peak morning rush hour, but it highlights the usefulness of network analysis and average travel time as a metric [27].

Depending on what type of network is being analyzed, there are various useful metrics that can be used to evaluate its functionality and resilience. Travel time is a useful metric, but it can be difficult calculate. It is dependent on speed limits, frequency of public transit, and congestion, among other variables [27]. Many analyses, this study included, use average shortest path as a metric because it gives similar information about the state of the network with fewer variables to determine, especially if the transportation network being analyzed is unimodal [24, 25, 26]. Using average shortest path distance to assess criticality does miss the effect of congestion on a network's performance, but this is acceptable to many applications of graph theory analysis, depending on the priorities of the research [28].

For some networks, a problem can arise when the removal of a node from the graph causes the network to be disconnected. In a fully connected graph, there is a path between any node and all other nodes in the network; this is not the case in a disconnected graph. Disconnected graphs form two or more subgraphs, as shown in Figure 6. The shortest path between any pair of nodes on different subgraphs becomes infinite. When this happens, researchers advocate using a metric called *inverse average shortest path distance*, which is calculated in the same way as the average shortest path distance from Equation 3 but with the infinite values replaced by zeros [20, 24, 26]. A decrease in inverse average shortest path distance corresponds to a decrease in network performance as more and more pairs of nodes become disconnected.

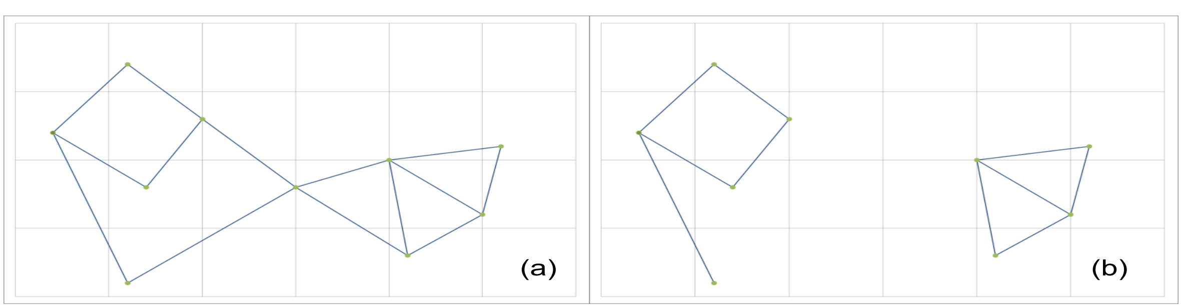

Figure 6: (a) Fully Connected Network, and (b) Disconnected Network Resulting from Node Removal

Several studies have been performed using graph theory and network science to evaluate the resilience of transportation networks. One study evaluated the rail and road networks in Florida, modeling rail stations and intersections as nodes. The criticality of the nodes was then ranked according to their betweenness centrality values. This ranking was used to remove nodes from the network to simulate a disturbance, then the effect of removal on the average shortest path and on the diameter of the network was observed. The authors of this study do not offer a quantitative measure of resilience; instead they state that based on their observations the network is "relatively resilient to disruptions" [25].

A study of the transportation infrastructure in Melbourne, Australia, compared the resilience of three of the city's transportation modes: the train, tram and street networks. Travel time was used as the metric to assess the network's performance. A simplifying assumption was made to assign the same speed limit across the entire street network. Four different speed limits were modeled. The results of the study indicated that the tram system was the most resilient, followed by trains and then street travel. The researchers did not offer quantitative values for resilience but did recognize that the resilience of the street network was dependent on the speed limit, with higher speed limits leading to lower resilience [29]. These qualitative assessments are certainly useful for some applications but in-depth transportation planning requires a more detailed, quantitative result.

Some researchers have developed graph theory methods to study transportation infrastructure resilience that yields quantitative results. Ip and Wang model the transportation network connecting several cities, with cities as nodes and the routes along different travel modes that connect them as links. The authors introduce weighting in their model by assigning node size according to city population and assigning the links a *reliability score*. This reliability score is between 0 and 1 and represents the probability that at any given time there will be a disturbance at that link, rendering it unusable. They also introduce the concept of *independent paths*. There can be an infinite number of paths through a network connecting a pair of nodes; paths are said to be independent if they do not require traveling along a link used by another path connecting the same pair of nodes. There are a finite number of independent paths connecting every pair of nodes [30].

Ip and Wang define the resilience of each node as the weighted sum of the number of reliable independent paths connecting it to all other nodes in the network. For example, if a node has a resilience value of 2.25, there are about 2 independent paths between it and every other node. Resilience of the entire network is the weighted average of the resilience of each node [30]. While this is a useful result, it requires knowledge of the type of transportation network being analyzed to be meaningful. A resilience value of 2 would likely be sufficient for a rail network, but indicates a lack of connectivity in an urban environment with several available travel modes.

Another concept introduced by Ip and Wang is *friability*. Friability is a measure of the reduction in the network's resilience due to the removal of a node or link. Friability can also be used as a method of ranking criticality of nodes and links. The elements with the highest friability are the most critical to the operation of the network, as their elimination has the greatest impact on the network's resilience [31].

The study discussed above added weighting to the network's nodes, but weighting can also be added to links. This study will use weighted links. A study of the worldwide airport network included 3,880 nodes (airports) and almost 19,000 links (direct flights operating during one calendar year). The analysis also included data on the distance between each pair of airports with a direct flight link and the number of available seats on each route. The authors recognized that the weight assigned to each link should be a function of the link's most important characteristics: distance and available seats. As the number of available seats increases, the effective distance between the nodes decreases because more seats enable more frequent and faster travel between the two locations [32]. They use Equation 5, shown below, to determine the weight of each link.

$$w_{ij} = \frac{d_{ij}}{s_{ij}} \qquad [32]\ (5)$$

where $w_{ij}$ is the weight o the link that connects nodes *i* and *j*, $d_{ij}$ is the distance between nodes *i* and *j*, and $s_{ij}$ is the number of available seats on direct flights connected nodes *i* and *j.*

## Methodology

Using the methodology and parameters of graph theory to study transportation networks and their resilience outlined in the previous section, this section will outline the steps taken in this study to incorporate weighted links into the methodology. Before the method was applied to the network of major state and federal highways in Albemarle County, Virginia, a smaller, simpler example network was analyzed to highlight the method and illustrate it in a manageable way. This section will also explain the development of the Albemarle County network and the tools used to build it and perform the analysis.

*Example Network*

The network shown in Figure 7 was analyzed as an illustrative example prior to performing the analysis on larger, more complex networks. Three network properties – link density, average node degree, and average shortest path distance – were used to show how the analysis functions.

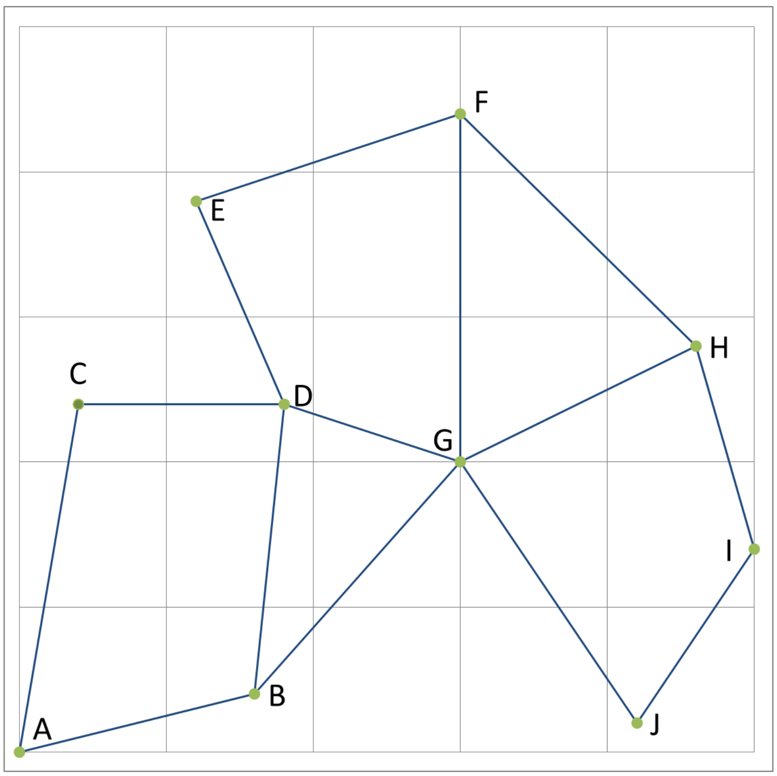


Figure 7: Example Network

Link density and average node degree are calculated using Equations 1 and 2, respectively. For this network, the link lengths are included in the shortest path calculations. The location of each node on the grid is used to determine the length of each link. Each gridline in Figure 7 represents 5 units. For example, the link connecting nodes C and D measures 7 units in length. The average shortest path distance was calculated using Equation 3.

To analyze the response of the network to a disturbance, nodes will be removed from the network and the arithmetic properties will be recalculated. Because the network is small and consists of only 10 nodes, the illustrative example contains three rounds of analysis: the first with all nodes operational, the second with one node removed, and the third with one additional node removed for a total of two nodes removed.

Two node removal strategies were used: random node removal (RNRS) and targeted node removal (TNRS). RNRS simulates disturbances such as weather events that are equally as likely to affect any point in the network, while TNRS can simulate an intentional attack on a specific point in the network. For RNRS, a random number generator determined the nodes to be removed. Node F was removed first, followed by Node H. Using TNRS, nodes are removed in order of node degree from highest to lowest. Node G, with degree 5, was removed first. Node D, which had a degree of 3 after the removal of node G, was removed next. The arithmetic properties for the network with all nodes and with selected nodes removed are shown in Table 2 below.

Table 2: Arithmetic Properties of Example Network

| RNRS | | | |
|---|---|---|---|
| Node(s) Removed | Link Density | Average Node Degree | Average Shortest Path Distance |
| n/a | 0.311 | 2.8 | 8.89 |
| F | 0.306 | 2.44 | 8.84 |
| F, H | 0.321 | 2.25 | 9.07 |
| TNRS | | | |
| G | 0.25 | 2 | 13.27 |
| G, D | 0.214 | 1.5 | 3.92 |

To see how the network is responding to the disturbance of node removal, the properties are plotted against the percentage of nodes removed, shown in Figures 8, 9, and 10 below.

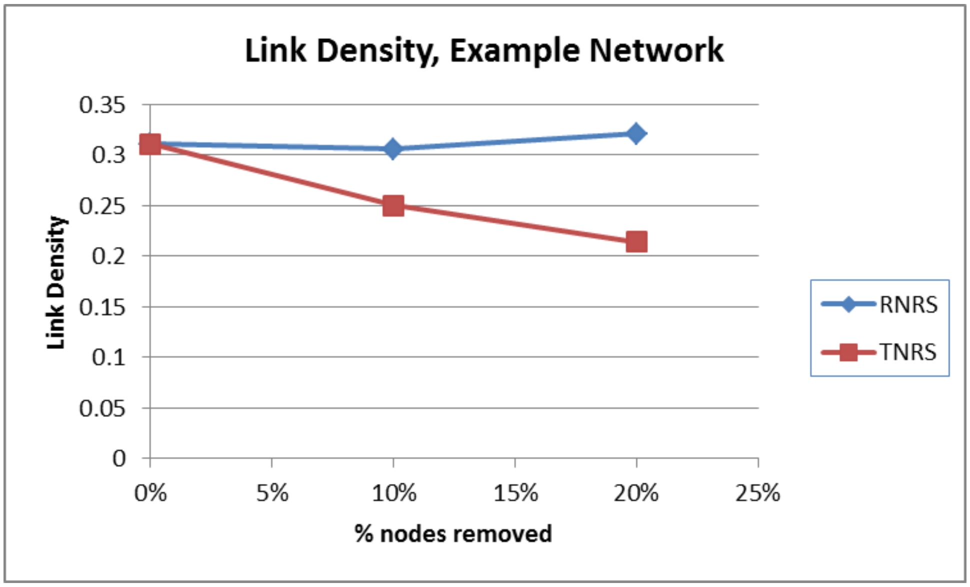

Figure 8: Link Density Response for Example Network

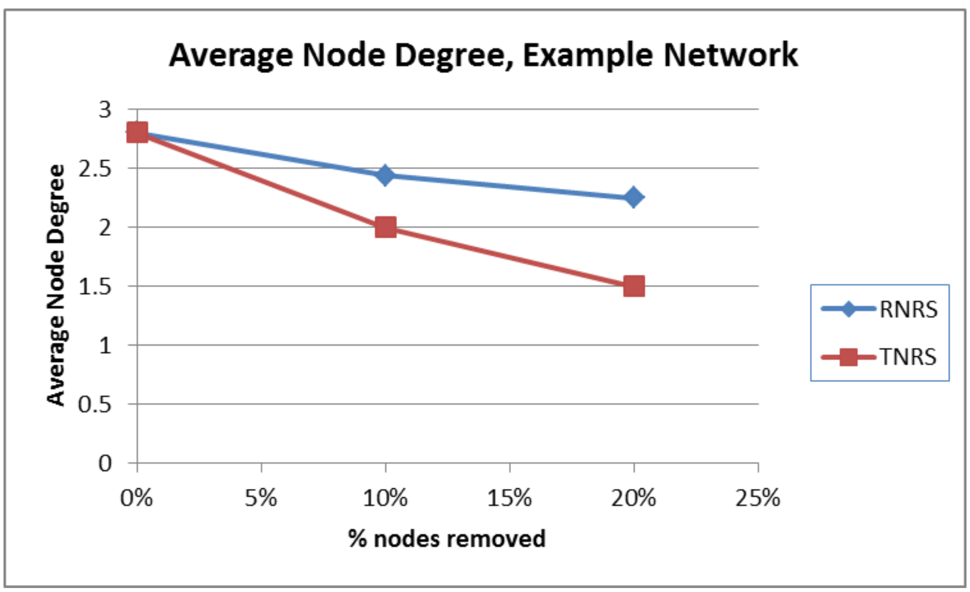

Figure 9: Average Node Degree for Example Network

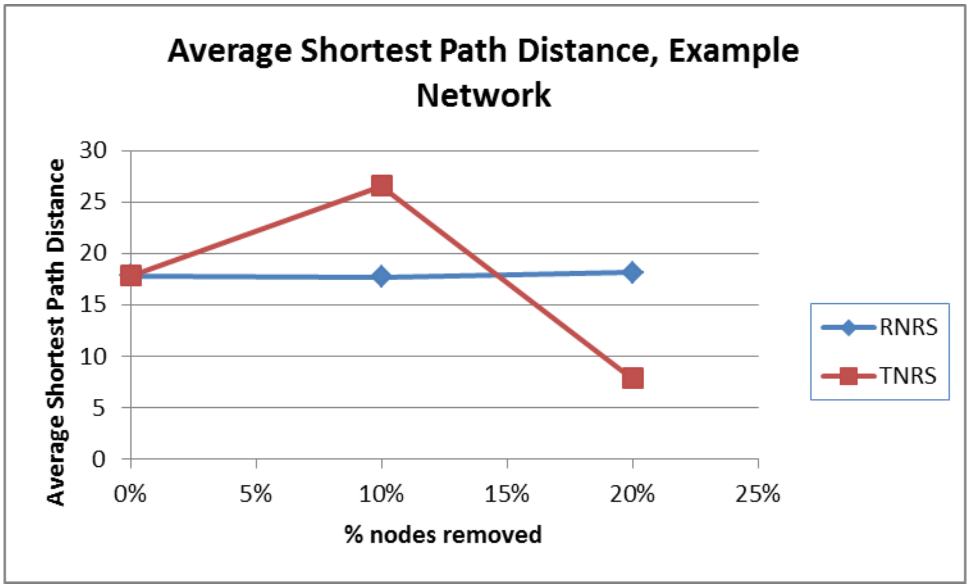

Figure 10: Average Shortest Path Distance for Example Network

Figure 10 shows an intersection of the two average shortest path distance curves at approximately 15% node removal. This point of convergence is called the *critical point* and represents the point at which the system has the same reaction to both node removal strategies. The network is resilient up to that point; it loses resilience to disturbance once more than that percentage of nodes has been removed [33, 34]. This value is the network's resilience index. For this example, the network is resilient to external shock as long as the disturbance removes less than 15% of the network's nodes. At any higher percentage of node removal, the system loses efficiency and is said to not be resilient.

The link density and average node degree curves in Figures 8 and 9, respectively, do not intersect. This is due in part to the small size of the example network. Depending on the metric and the type of network being analyzed, it's possible that the curves on plots such as the ones shown here will never intersect. When this occurs, the resilience index is determined from plots using metrics where the curves do intersect.

*Albemarle County Highway Network*

Finally, the method illustrated here was applied to a considerably more complex network, the highway system of major federal and state highways in Albemarle County, Virginia.  The network consists of 10 routes totaling 176 miles of roadway, and all routes allow traffic in both directions.  A map of the included routes is shown in Figure 11.

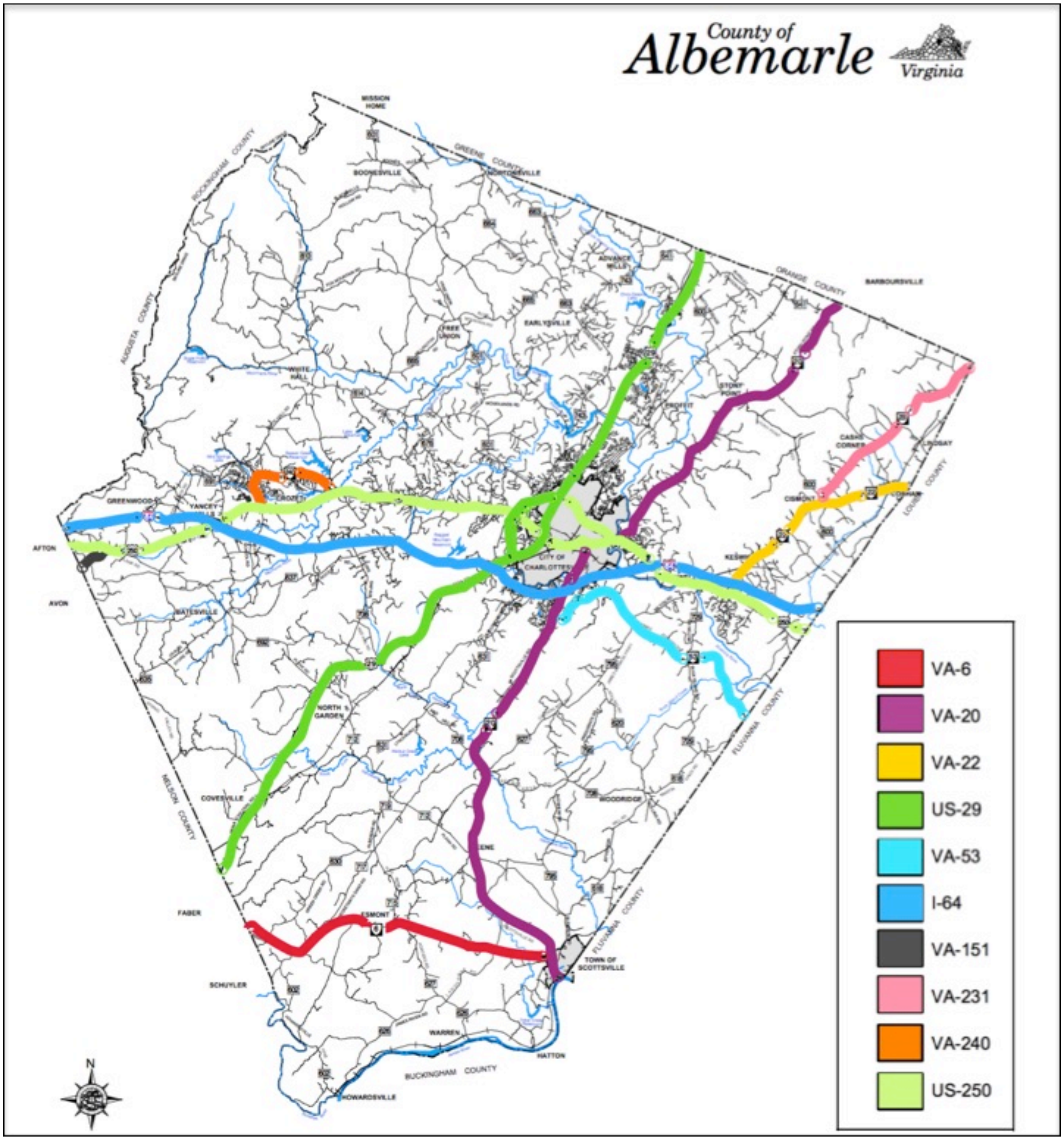

Figure 11: Map of Albemarle County Roads Analyzed

The goal of this example is to illustrate how this method can be used to evaluate the resilience of a transportation infrastructure system. Specifically, the effect of bridge outages on a highway system was investigated here. Nodes were placed at the location of bridges along the selected routes. The National Bridge Inventory was used to identify bridges along the routes shown in Figure 11, and the GIS tool ArcMap was used to show their location. All roadway sections were modeled as undirected links. Twin bridges were modeled as a single node. The analysis was performed in Matlab. Due to the nature of Matlab's built-in network analysis tools, nodes were also placed at the intersections between two routes, and between a single route and the Albemarle county line. However, because the goal of this study was to evaluate the effect of bridge outages, only the nodes representing bridges were removed during the analysis.

The network studied is shown in Figure 12; it has 80 nodes, 57 of which represent bridges, shown in purple, and 23 intersections, shown in orange. More information about the bridges and intersections are given in Appendices A and B, respectively. The network has 86 links of various lengths. ArcMap was also used to determine the length (in miles) of each link in the network. A list of the links including the length of each is given in Appendix C. Matlab assumes all links in a network have a length of 1 unless otherwise specified. This can be altered by adding a weight to each link, which the program treats as a distance [35]. The analysis was first performed with link lengths included.

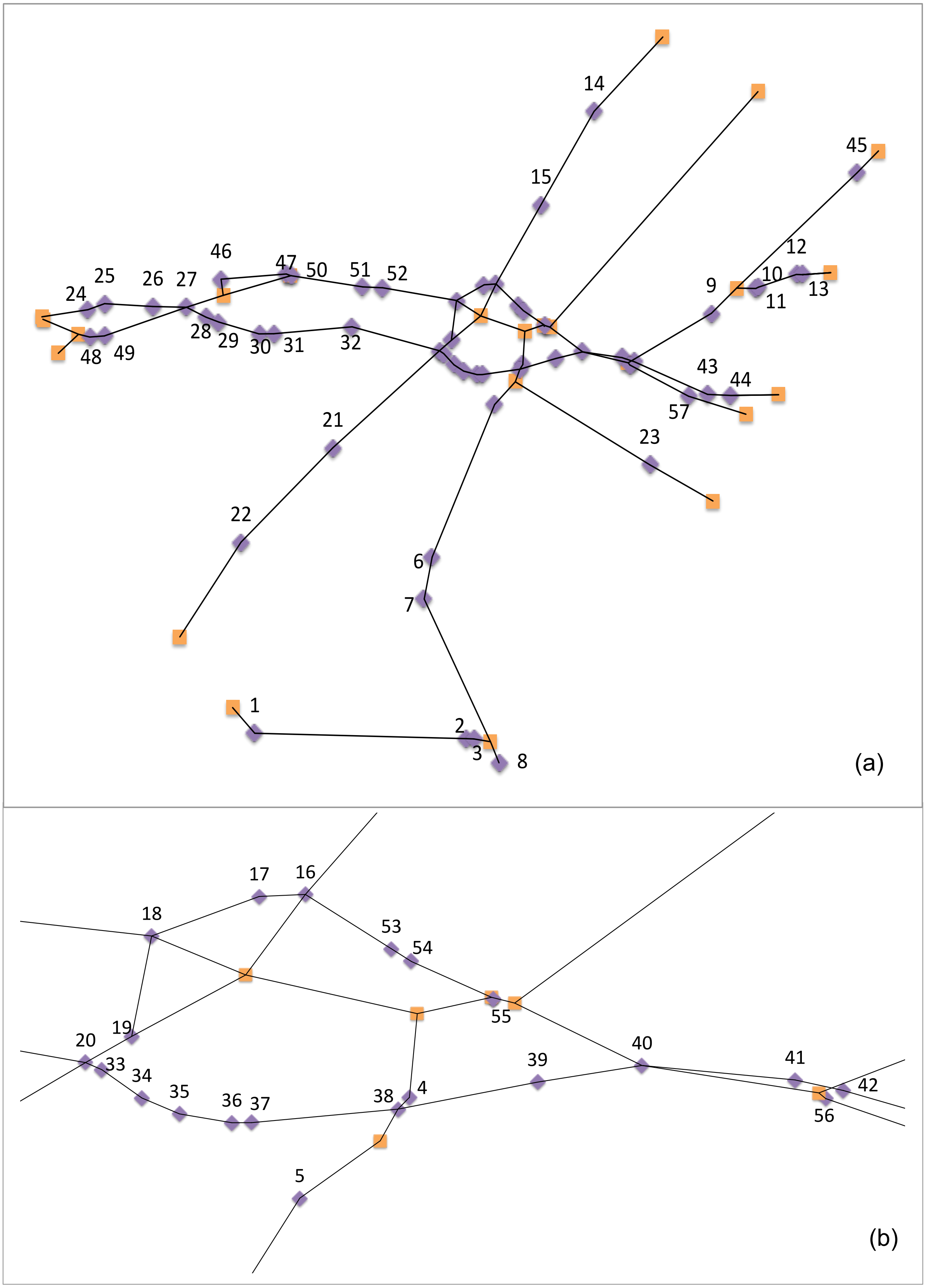


Figure 12: (a) Map of Albemarle County Highway Network, and
(b) Enhanced View of Charlottesville to Show Detail

The goal of this study is to evaluate the effect that adding weight to links has on the network's parameters. Weights were assigned according to the importance of each link. To model the importance of each roadway section in Albemarle County, annual average daily traffic (AADT) data was used. AADT counts are from 2014 and were published by the Virginia Department of Transportation (VDOT) [36]. VDOT reports AADT for sections of the roadway of various lengths. The boundaries of these sections were either a county line or an intersection with another road. These boundaries did not always align with the bridge locations. Where they did, the AADT for those links is precisely known. For the roadway sections where the VDOT sections did not match the links in the studied network, a weighted average was taken to estimate the AADT. The AADT values computed for each link are shown in Appendix C.

Because weights had already been added to the links to represent the link lengths, these weight values were altered to incorporate AADT data. Two methods were used to accomplish this. The first altered the weight value directly proportional to AADT, and the second considered the order of magnitude of the AADT. Formulas for the altered weights are shown in Equations 6 and 7 below.

$$\text{Altered Weight 1} = \frac{Link\ Length}{\left(\frac{AADT}{1{,}000}\right)} \tag{6}$$

$$\text{Altered Weight 2} = \frac{Link\ Length}{\log_{10}(AADT)} \tag{7}$$

The values for each link weight for both weighting schemes are shown in Appendix C.

With the networks created, average shortest path distance, diameter, link density, and average node degree were calculated for each. Then, nodes were removed using RNRS and TNRS. For RNRS, a random number generator determined the order of node removal. Two strategies were used for TNRS, both using betweenness centrality to rank nodes. The first, TNRS-a, involved removing nodes based on the node ranking of the initial network. For the second method, TNRS-b, the betweenness centralities were recalculated after each node removal to determine the next node to be removed. After each node removal, the four properties were recalculated.

## Results and Discussion

This section presents the results for the unweighted Albemarle County highway network and for the two weighting schemes tested. In all plots shown in this section, the values were normalized to show the change from each property's value before any nodes were removed. The blue series, RNRS, shows data for node removal based on a random number generator. The red series, TNRS-a, shows data for node removal based on the betweenness centralities of the original network. The method involving recalculating betweenness centralities after every node removal is shown by TNRS-b, the green series. The first green data point shown is the last point before the two TNRS strategies diverge.

The unweighted network considered only the distance between each node in the analysis. Weighted Network 1 modified the weight directly proportional to AADT using Equation 6, while Weighted Network 2 considered the order of magnitude of AADT using Equation 7.

### *Unweighted Network*

This section presents the results for the unweighted network, which includes the link lengths in the analysis.

**Average Shortest Path Distance**

Figure 13 shows the average shortest path distance results for the unweighted Albemarle County highway network.

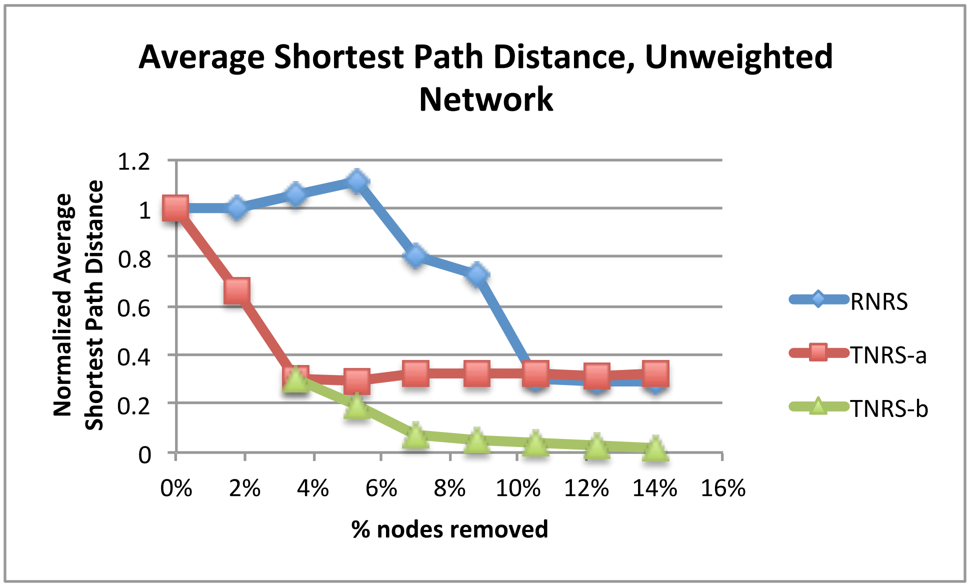


Figure 13: Average Shortest Path Distance for Unweighted Network

The RNRS and TNRS-a curves intersect at around 10.5% of nodes removed. This indicates that the Albemarle County highway network is resilient to external shocks as long as the event disturbs fewer than 10.5% of the network's bridges. If an event renders more than 10.5% of the studied bridges unusable, the network loses functionality and is not resilient.

The TNRS-b does not intersect with either other curve after it diverges from the TNRS-a curve. Instead, it quickly falls to near zero after about 7% of the nodes are removed. This suggests that the network is not resilient to a sophisticated targeted attack and that the system would be effectively shut down shortly after such an event.

The RNRS curve increases through the first three node removals. This occurs because none of those three nodes divided the network into disconnected subgraphs. The first three nodes removed were 47, 52, and 35. These nodes represent bridges on

VA-240 east of Crozet, US-250 between Crozet and Charlottesville, and I-64 between US-29 and VA-20, respectively. Their locations are shown in Figure 14 below in blue. The orange nodes representing intersections are not shown in any network images in this section. With these nodes removed, the network was still fully connected, and a path existed between every pair of remaining nodes. The shortest paths that previously used these nodes were rerouted and their length increased, leading to the increase in average shortest path distance for the entire network.

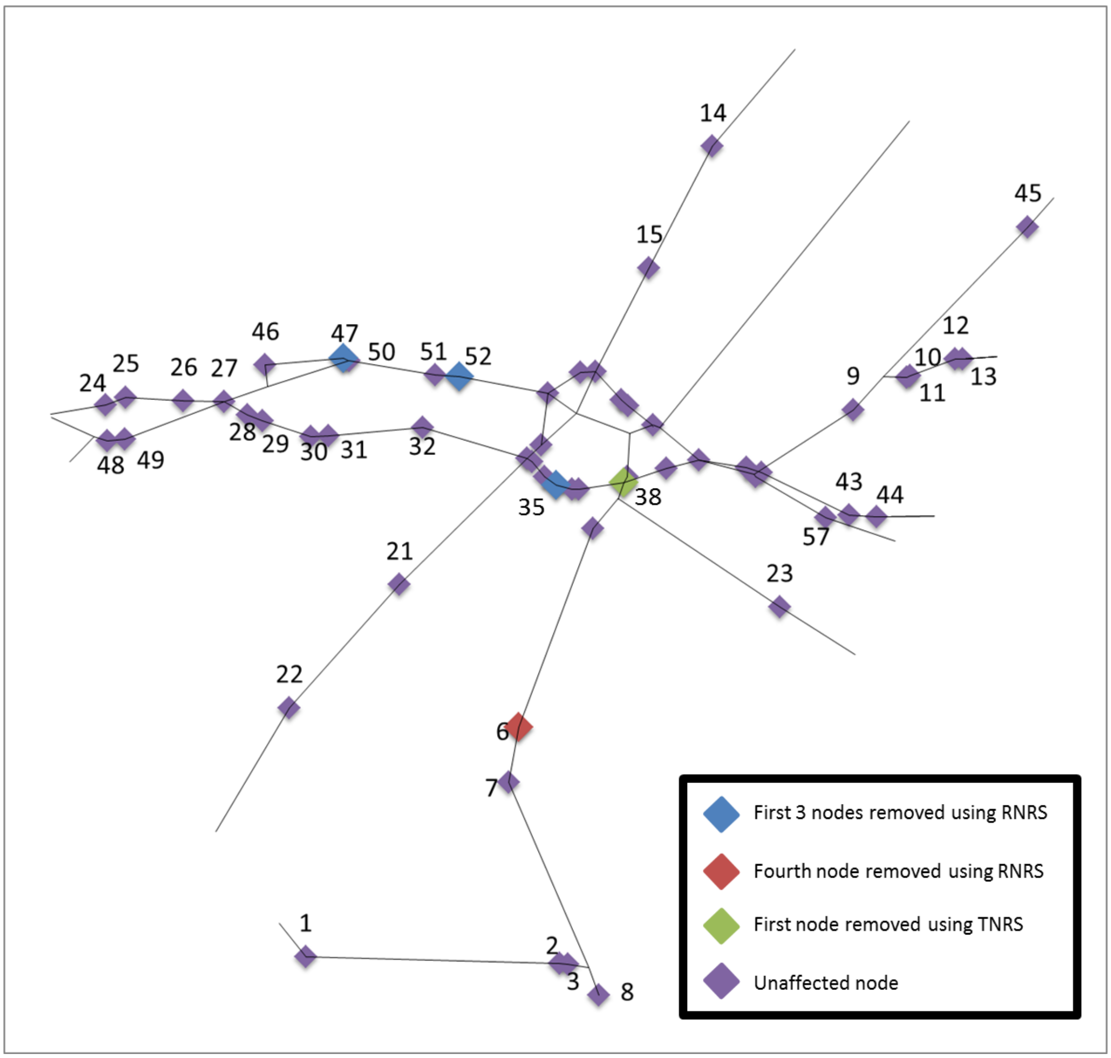

Figure 14: Location of Removed Nodes

With the fourth node removal, the average shortest path distance began to decrease. The fourth node removed, 6, represents a bridge on VA-20 south of Charlottesville, and its location is shown in red in Figure 14. While not one of the most centrally located nodes in the network, its removal created two separate subgraphs and disconnected the Scottsville area and the entire stretch of VA-6 in Albemarle County from the rest of the network, shown in Figure 15. The average shortest path distance plot is shown in the upper left of Figure 15, and the orange highlighted area shows the drop in average shortest path caused by the node elimination shown in the figure.

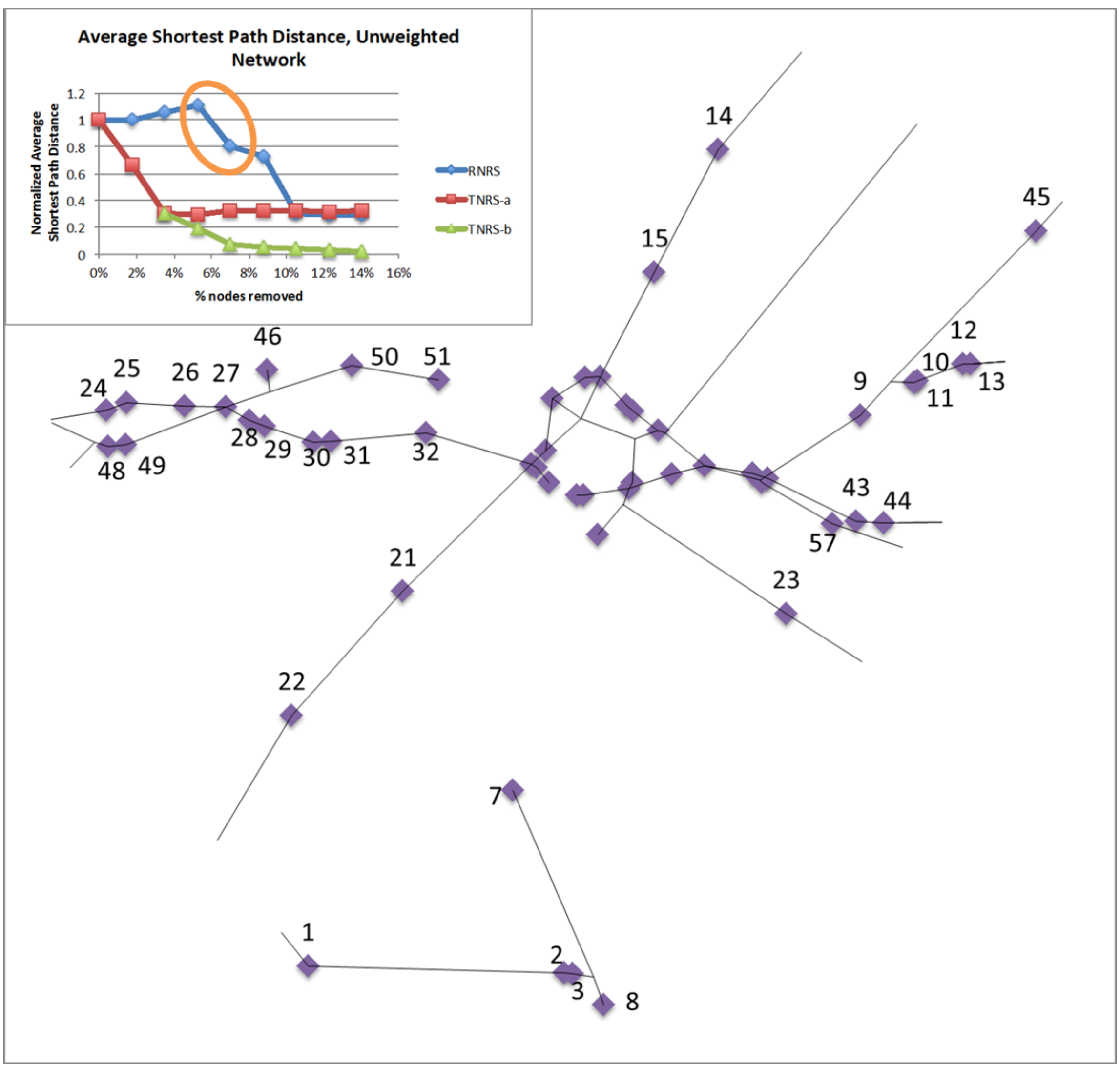

Figure 15: Disconnected Subraphs due to Removal of Nodes 47, 52, 35 and 6

There is no longer a shortest path connecting every pair of nodes in the network, and the path distance between disconnected nodes becomes infinite. These infinite values were replaced with zeros to give the average inverse shortest path distance. A decrease in the average inverse shortest path distance indicates loss of network functionality as more and more path distances become infinite and are replaced with zeros.

The first node removed using both targeted node removal strategies is node 38, representing a bridge that forms the intersection between I-64 and VA-20. Its location is shown in green in Figure 14, and the resulting disconnected subgraphs are shown in Figure 16. Because the network is now disconnected, the average inverse shortest path is used. The upper left corner of Figure 16 highlights the decrease in average shortest path distance caused by this node's removal.

The red TNRS-a curve decreases sharply with the first two node removals and then levels out beginning with the third node removal. After the second node removal, the original network has been separated into three disconnected subgraphs, shown on the left of Figure 17.

The leveling-off effect is seen because the nodes are removed based on the initial betweenness centrality ranking. Node 4 is the third node removed in TNRS-a because it originally has a high betweenness centrality. After node 38 is removed, node 4 is left with only one link connected to it. When node 4 is removed, there is not much effect on the network because the node's degree was only 1. This effect continues through TNRS-a and explains the flat section of the data after the third node removal highlighted in the bottom center of Figure 17. Even after six additional nodes are

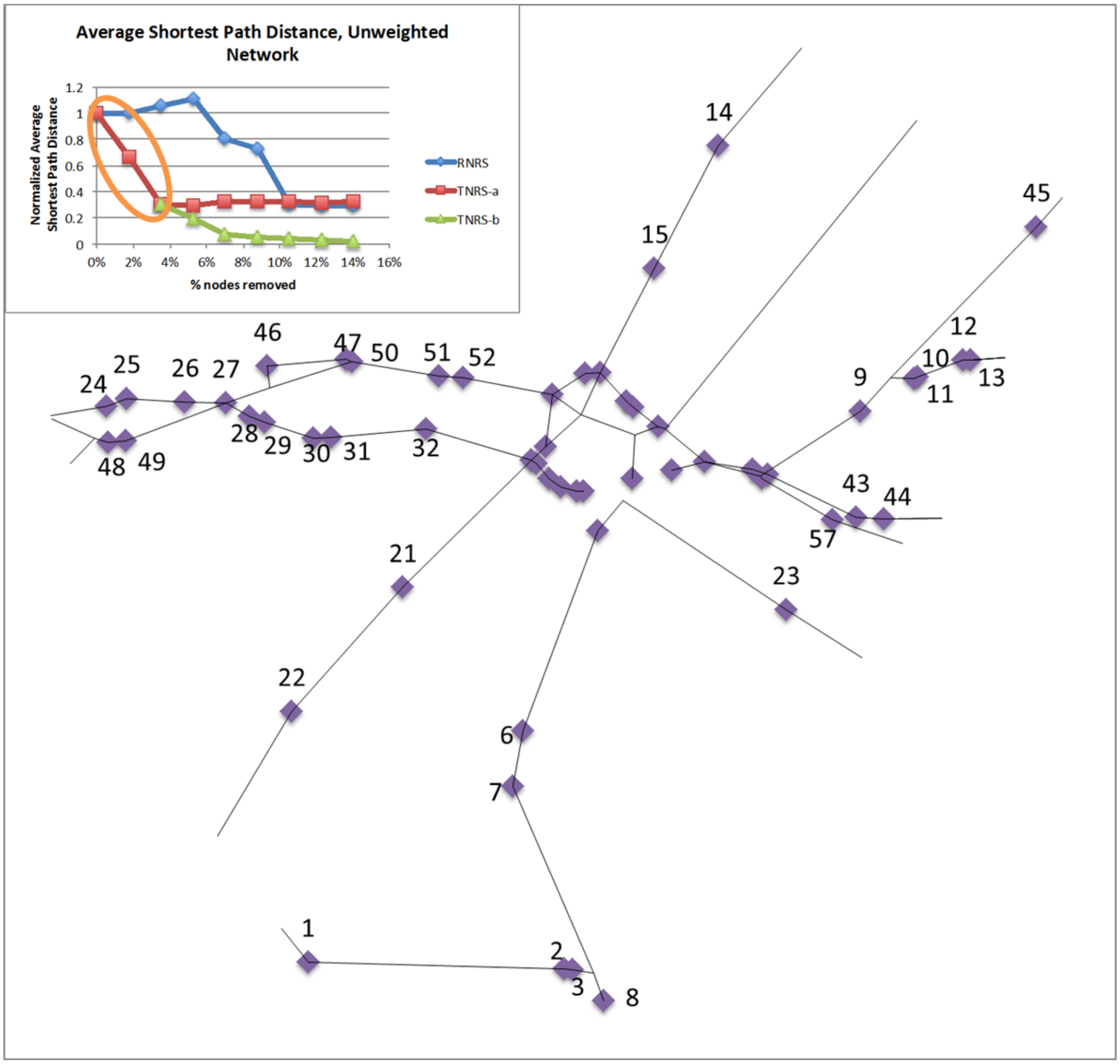


Figure 16: Disconnected Subgraphs due to Removal of Node 38

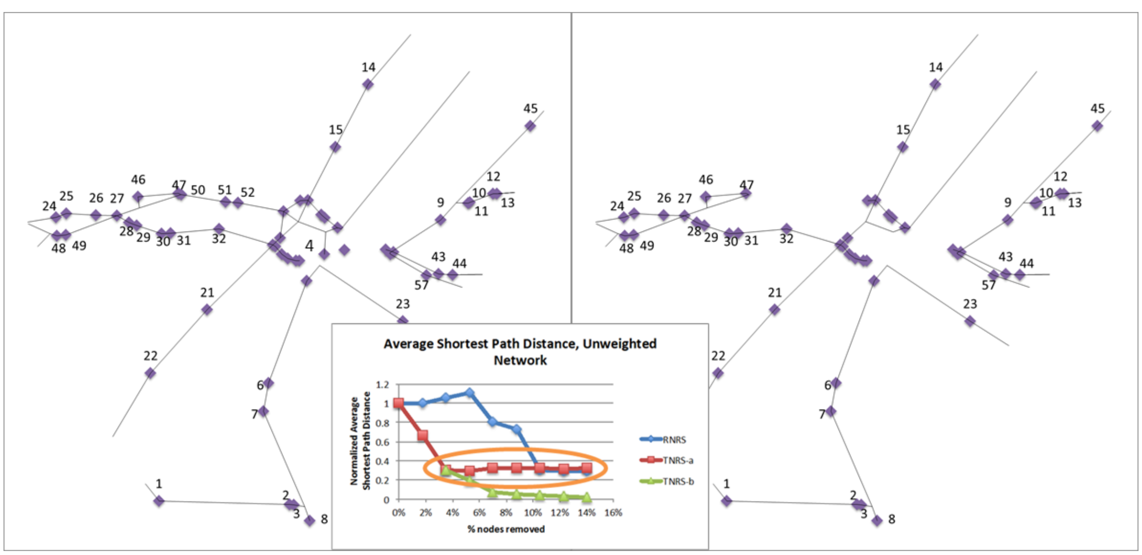


Figure 17: Disconnected Subgraphs due to TNRS-a

removed, the network is still comprised of the same three subgraphs, shown on the right of Figure 17. A difference between the two networks is visible, but no additional disconnected subgraphs have been created.

A flat section is not seen in TNRS-b because the betweenness centralities are recalculated after each node removal to maximize the detrimental effect on the network. After all eight rounds of node removal using TNRS-b, the network has been divided into 12 disconnected subgraphs, shown in Figure 18. This is why the TNRS-b data decreases throughout the analysis.

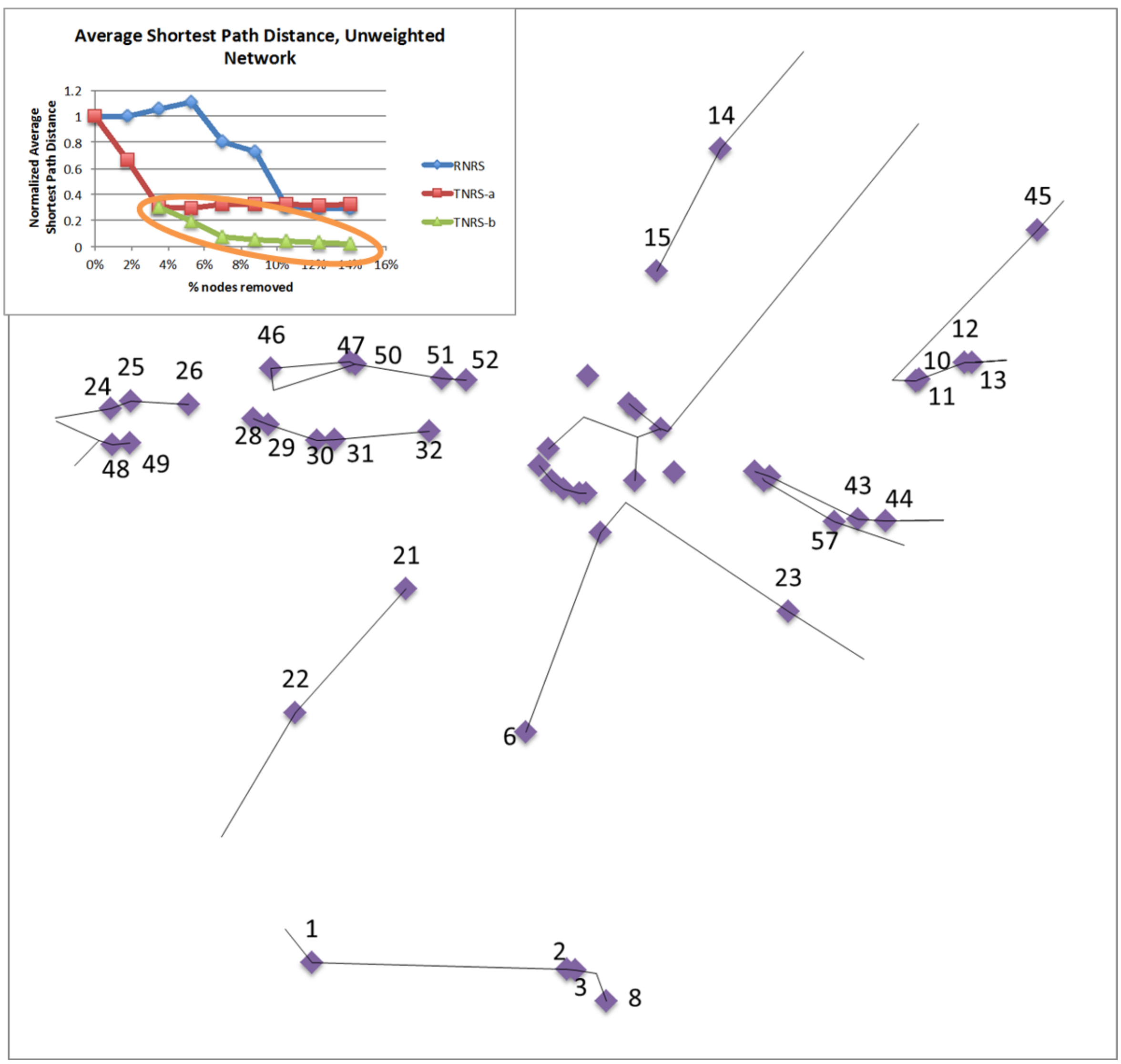


Figure 18: Disconnected Subgraphs due to TNRS-b

**Diameter**

Diameter calculations for the unweighted network are shown in Figure 19 below.

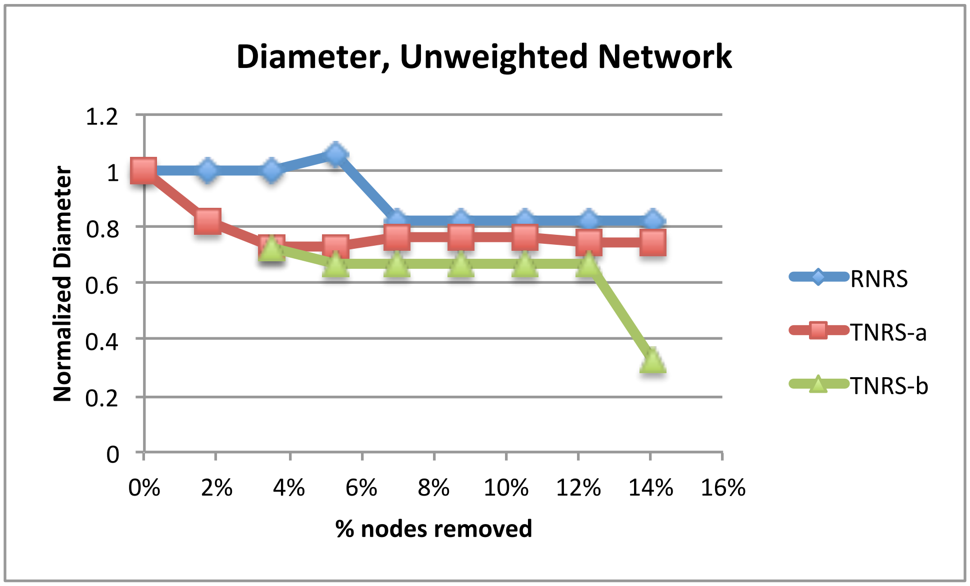


Figure 19: Diameter for Unweighted Network

The network's diameter is the shortest path distance for the pair of nodes that are farthest apart, so not every node removal will cause a change in the network's diameter. If the node removed is not on the shortest path connecting the pair of nodes that are the farthest apart, the network's diameter will likely not be affected. This explains the long periods of constant diameter in the plot above.

The exception occurs when a node with high betweenness is removed if that node is not on the diameter's path. Removal of a node with high betweenness requires the network to reroute many shortest paths, making them longer. One of these new shortest paths may be longer than the network's existing diameter, increasing the value of the property. This is the cause of the increase in diameter on the blue RNRS curve seen at around 6% of nodes removed and is due to the third node removal.

Any decrease in the network's diameter is a sign that the node removal divided the network into disconnected subgraphs. This is similar to the cause of decreases in the average shortest path distance when the network becomes disconnected. The path distance between the pair of nodes that are the farthest apart becomes infinite in a disconnected graph, and its value is replaced by zero. The diameter of a disconnected graph is essentially the diameter of its largest subgraph, leading to the decreases seen in Figure 19.

The diameter curves do not intersect, so the critical point for the unweighted network is not as clear as it was using average shortest path distance. The difference between diameter values in the first few rounds of node removal was not as pronounced as the difference in average shortest path distance between curves, highlighted by the comparison of the two plots shown in Figure 20.

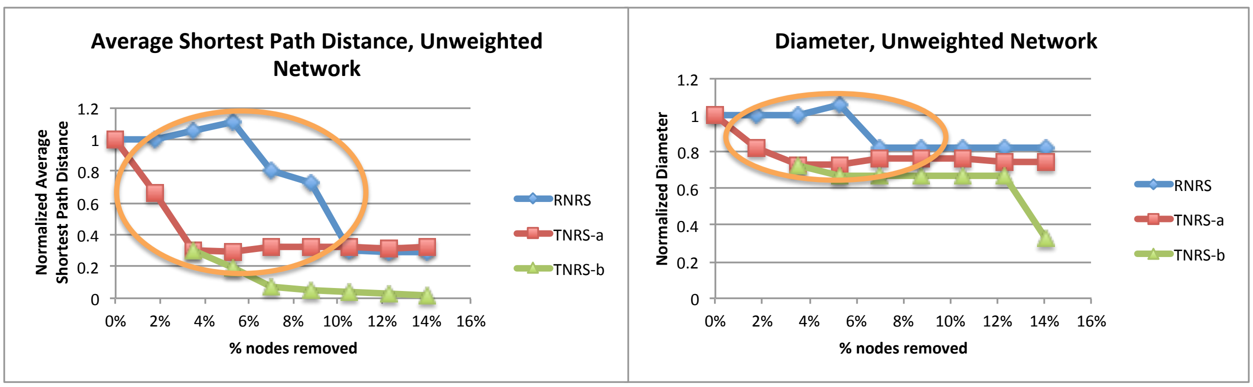


Figure 20: Comparison of Average Shortest Path Distance and Diameter Plots for the Unweighted Network

At around 7% of nodes removed, the RNRS and TNRS-a diameter curves are within 7.5% of each other. This is the critical point for the network, indicating that the network is resilient to external shock as long as fewer than 7% of nodes are removed. This is below the resilience index of 10.5% found when using average shortest path distance. In this case, using diameter leads to a decreased resilience index for the same network.

## Link Density and Average Node Degree

Figures 21 and 22 show the results for link density and average node degree, respectively, for the unweighted network.

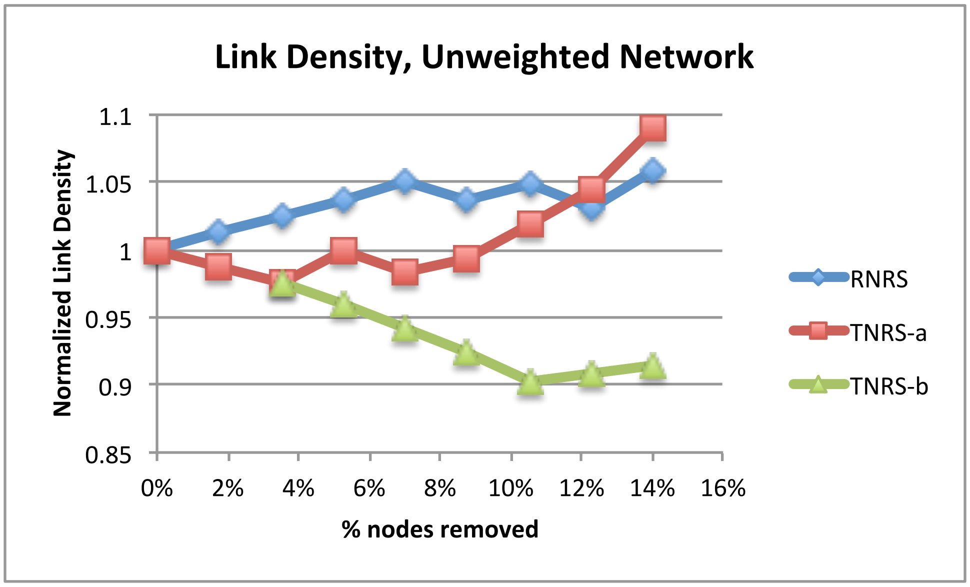


Figure 21: Link Density for Unweighted Network

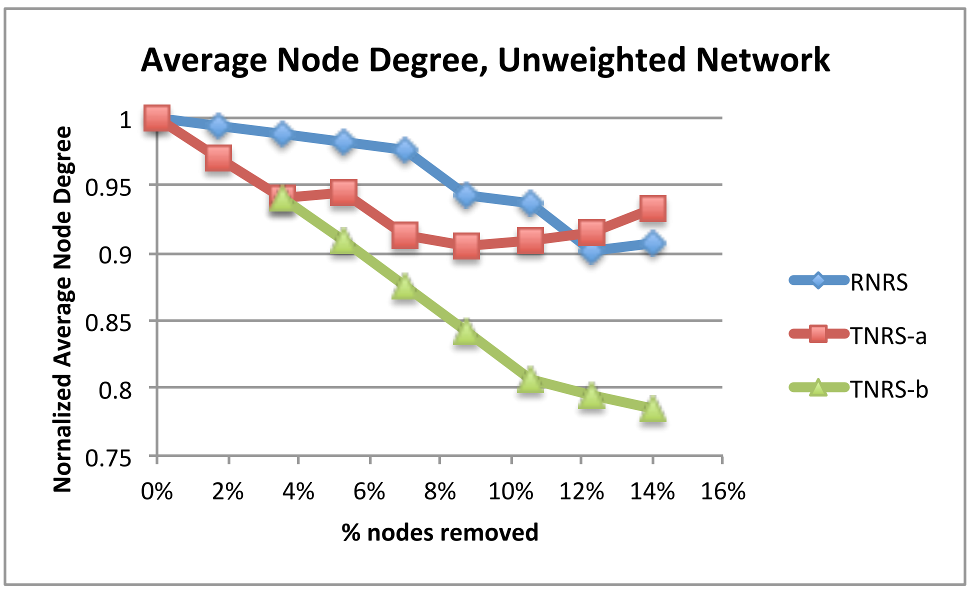


Figure 22: Average Node Degree for Unweighted Network

Both plots show an intersection between the RNRS and TNRS-a curves at 12% nodes removed. However, these do not represent the network's critical points. Link density and average node degree are useful network properties in many modeling scenarios and should be included in the analysis of various transportation infrastructure systems. However, for the highway system being modeled here, with bridges as nodes and roadway sections as links, these metrics are not as useful as the two previously discussed.

Link density is a measure of how connected the network is. The network's link density is the proportion of the number of links in the network to the maximum number of links the network could support if every pair of nodes in the network was connected by a single link. Transportation infrastructure networks, including highway systems like the one studied here, are generally not designed to have high link density, and it would be impractical to do so. Link density is not as useful a metric as diameter or average shortest path distance.

Similarly, average node degree is not the best metric to consider when modeling a highway system in the way done in this study. Because the system models bridges as links, the majority of the nodes will have a degree of 2, representing the roadway that extends beyond the bridge in both traffic directions. The exception is bridges that located at intersections of two routes in the model, where it is assumed that a disruption to the bridge would disrupt traffic on both the route carried and the route crossed. In the Albemarle County network, only seven of the 57 nodes have this feature. Average node degree would be a more appropriate metric when considering other transportation infrastructure systems, such as airport networks or railway systems that are designed to have more than two links at each node.

Additionally, normalized link density and average node degree values calculated and shown in Figures 21 and 22 do not deviate from the original value as much as the average shortest path distance or diameter do. The RNRS and TNRS-a curves for average shortest path distance in Figure 13 drop to 30% of their original value, and the TNRS-b curve falls to practically zero. In comparison, the RNRS and TNRS-a curves for link density and average node degree remain within 10% of the original value in either direction. Only the TNRS-b curves fall significantly, but only to around 90% for link density and 78% for average node degree. This confirms that removing nodes based on recalculated betweenness centrality rankings leads to greater disturbance in the system. Plots for link density and average node degree will not be discussed for the weighted networks studied but are shown in Appendix D.

*Weighted Network 1*

This section shows the results of the analysis of Weighted Network 1, in which the link weights include link length and AADT data, calculated using Equation M6.

**Average Shortest Path Distance**

Figure 23 shows the average shortest path distance curves for Weighted Network 1 (WN1).

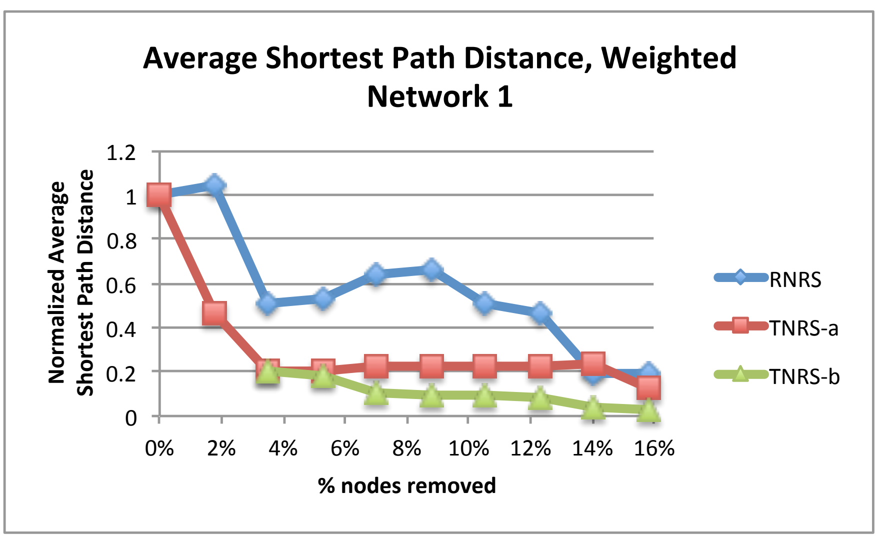


Figure 23: Average Shortest Path Distance for Weighted Network 1

The average shortest path distance plot for WN1 is similar to the same plot for the unweighted network in that the RNRS and TNRS-a curves intersect, but the TNRS-b curve does not intersect with either other curve.  The critical point at which the RNRS and TNRS-a curves intersect occurs at around 14% of nodes removed, indicating the system is resilient to external shocks as long as fewer than 14% of the network's nodes are eliminated.  This is higher than the unweighted network's value of 10.5%.  This indicates that including the AADT data into the weighting of the links using Equation 6 increases the resilience of the system.  Previously, using the unweighted network, the analysis was not able to take into account the importance of each route being studied. With AADT data included, the model is more complete.  It now has the capability to recognize that removing a bridge on a less traveled road such as VA-6, where the AADT is 1150, should not affect the network's properties as much as removing a bridge on a more popular route, such as the U.S. 29 bypass, where AADT reaches 50,000.

One notable difference between the unweighted and WN1 average shortest path distance plots is that the RNRS curve in WN1 drops significantly after the second node removal, whereas the same curve in the unweighted plot increases from its original value until after the fourth node removal.  The two plots are shown side-by-side in Figure 24 for comparison.

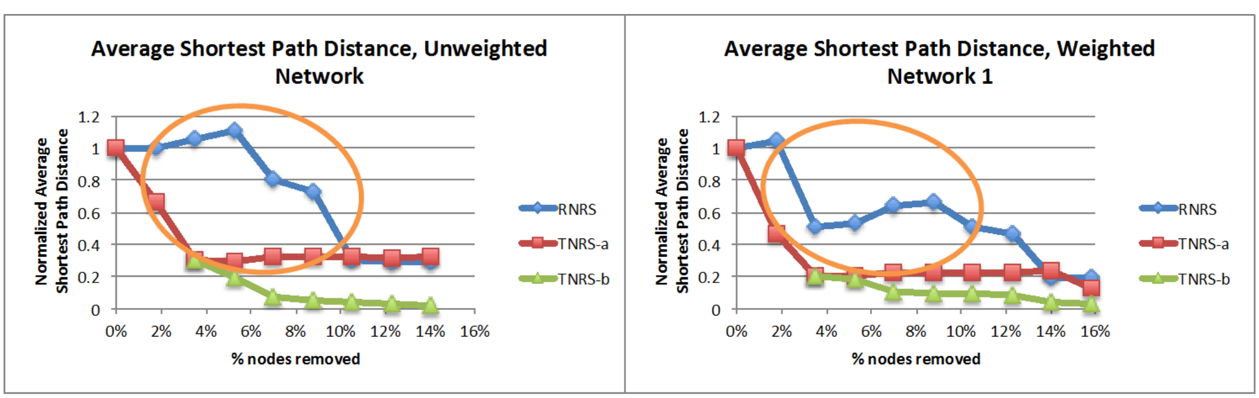


Figure 24: Comparison of Average Shortest Path Distance Plots for the Unweighted Network and WN1

The second node removed from WN1 using RNRS was node 6, a bridge on VA-22 south of Charlottesville, mentioned previously and shown in red in Figure 16. This is the same node that caused the drop in the RNRS curve for the unweighted network. The same phenomenon occurred for WN1: the node's removal created two disconnected subgraphs, leading to many shortest path values being replaced by zeros. However, with weighting included, the analysis was able to recognize that even though removing this node disconnected the network, it was not a very important node. The AADT of both links connected to that node is 7,000, which is on the low end of AADT values in the network. Later node removals did not further disconnect the network, and so increases in average shortest path distance were observed in the RNRS curve from the second node removal until the fifth, shown on the right in Figure 24.

**Diameter**

Figure 25 shows the diameter curves for WN1.

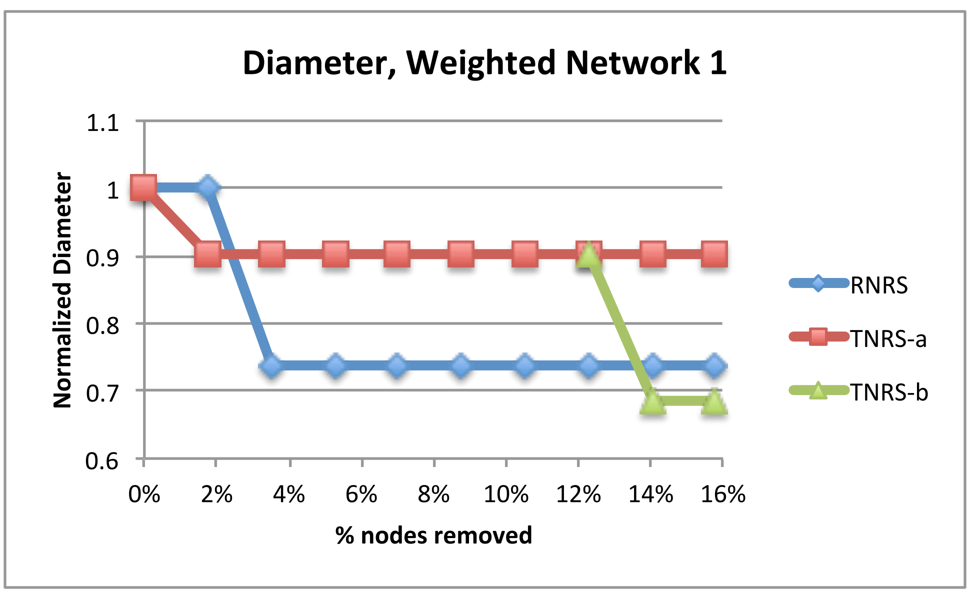


Figure 25: Diameter for Weighted Network 1

The RNRS and TNRS-a curves intersect at around 3% nodes removed. This would indicate that the network is resilient to external shock only as long as less than 3% of nodes are removed. This is much lower than 14%, the resilience index observed for WN1 using average shortest path distance. This phenomenon can be explained by a limitation in the weighting scheme used. The first node removed, 37, had no effect on the network's diameter. Node 6 was the second node removed. This node has been discussed previously and is shown in red in Figure 14. Its removal divides the network into two disconnected subgraphs, shown in Figure 26, with the corresponding drop in diameter highlighted in orange in the upper left. The southern subgraph includes the Scottsville area, the section of VA-20 south of Carters Mountain Road, and the entire section of VA-6 in Albemarle County.

The section of VA-6 connecting nodes 1 and 2 is 9.4 miles long. It is the second-longest link in the entire network. As previously discussed, VA-6 is the least-traveled road in the network, with an AADT of 1150. Because the weight of the link is the link's distance divided by its AADT, as per Equation 6, the weight of the VA-6 link becomes artificially inflated because the numerator is relatively large and the denominator is relatively small, leading to a larger link weight. With the network fully connected, the diameter's path traveled through node 6. With it removed, a different, shorter path becomes the network's diameter. This explains the sharp drop in the network's diameter after node 6 is removed. This same thing would have happened had any of the following nodes been removed instead of node 6: 1, 2, 3, 5, or 7. These six nodes are critical to the diameter analysis. It's likely that a different RNRS order would have yielded different results and that the blue RNRS curve in the upper left of Figure 26

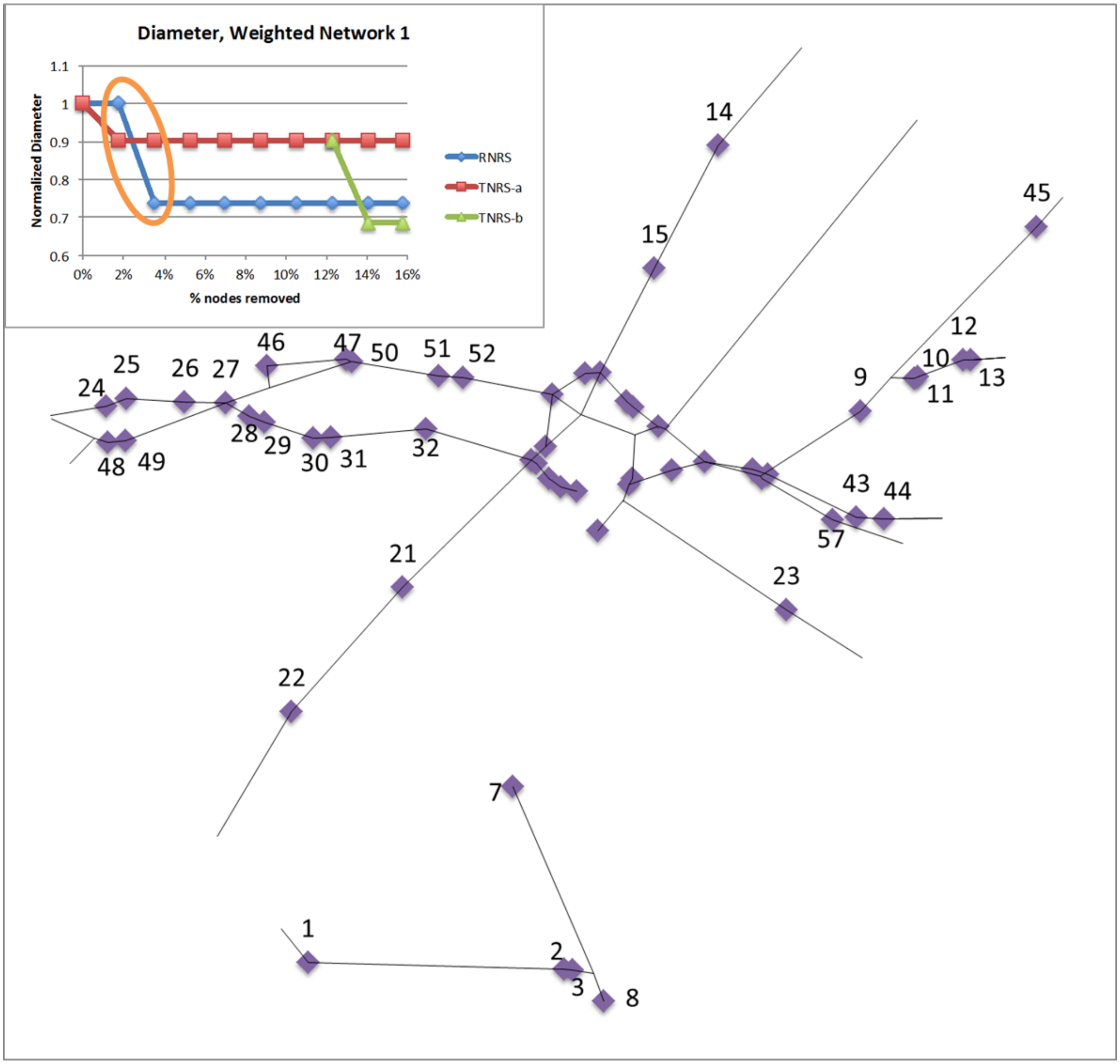


Figure 26: Disconnected Subgraphs due to Removal of Nodes 37 and 6

would have remained above the red TNRS-a curve, giving a different resilience index for the network closer to the 14% index observed by measuring average shortest path distance.

*Weighted Network 2*

This section shows the results of the analysis of Weighted Network 2 (WN2), for which the link weights include link length and AADT data, calculated using Equation 7.

**Average Shortest Path Distance**

Figure 27 shows the average shortest path distance curves for WN2.

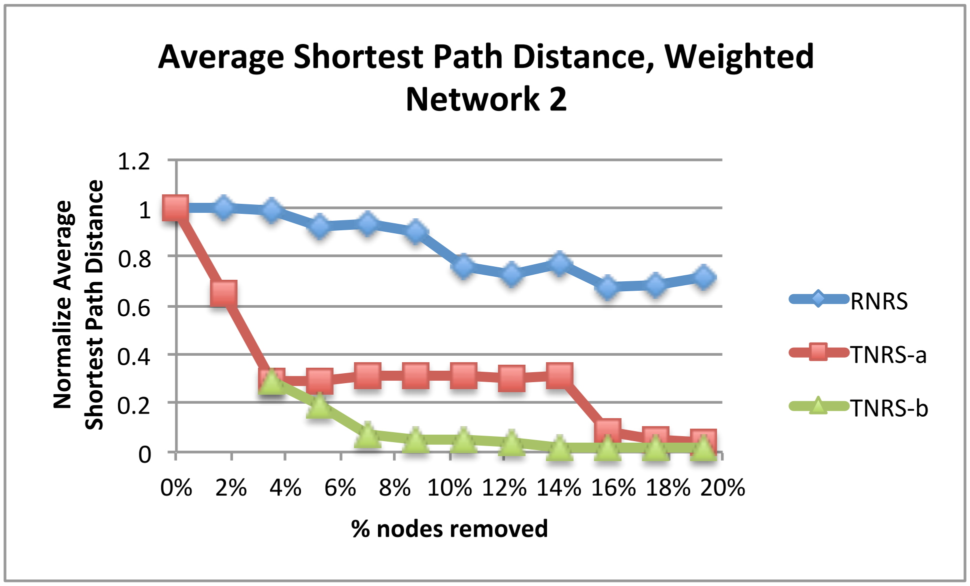


Figure 27: Average Shortest Path Distance for Weighted Network 2

The average shortest path distance plot for WN2 presents a special case because the RNRS and TNRS-a curves neither intersect nor come close enough to each other to determine the critical point of the network. The analysis was extended to include three additional rounds of node removal to bring the number of nodes removed to 11. This was done in an attempt to see if the curves would intersect. Instead of the extra round bringing the RNRS and TNRS-a curves closer together, it actually led them farther apart. After the 10th and 11th node removals, the RNRS values increased while the TNRS-a values decreased. At 19% nodes removed, the TNRS-a and TNRS-b curves had similar values, but both were practically zero, so this does not indicate a critical point. Additionally, comparing two different TNRS schemes is not as useful as comparing RNRS to TNRS when determining resilience index, because it is known that the TNRS-b curve will always be below the others.

The RNRS curve in Figure 27 does steadily decrease as more nodes are removed, but a sharp decrease like those seen in similar plots for the unweighted network and WN1 (Figures 13 and 23, respectively) is not seen here. Instead, the average shortest path distance never falls below 65% of its original value. In contrast, both TNRS curves fall to less than 30% of the original values after only two node removals. The TNRS-b curve quickly falls to near zero, and the TNRS-a curve also reaches that point later in the analysis. This indicates that the network is relatively resilient to random disturbances but very vulnerable to targeted attacks. This is one characteristic of a scale-free network. Some examples of scale-free networks are cells, the Internet, and social networks [37]. The node degree distribution of a scale-free network follows a power law distribution as opposed to being clustered around a mean. This leads to increased redundancy in the network and therefore a higher tolerance to random disturbance. However, due to the power law nature of node degree distribution, a few nodes will have very high degrees, and their removal could devastate the system [38]. Even though WN2 follows the same node degree distribution as the unweighted network and WN1, it behaves like a scale-free network when average shortest path distance is used as a metric. A resilience index of the type discussed in this study is not available for a scale-free network.

**Diameter**

Figure 28 shows the average shortest path distance curves for WN2.

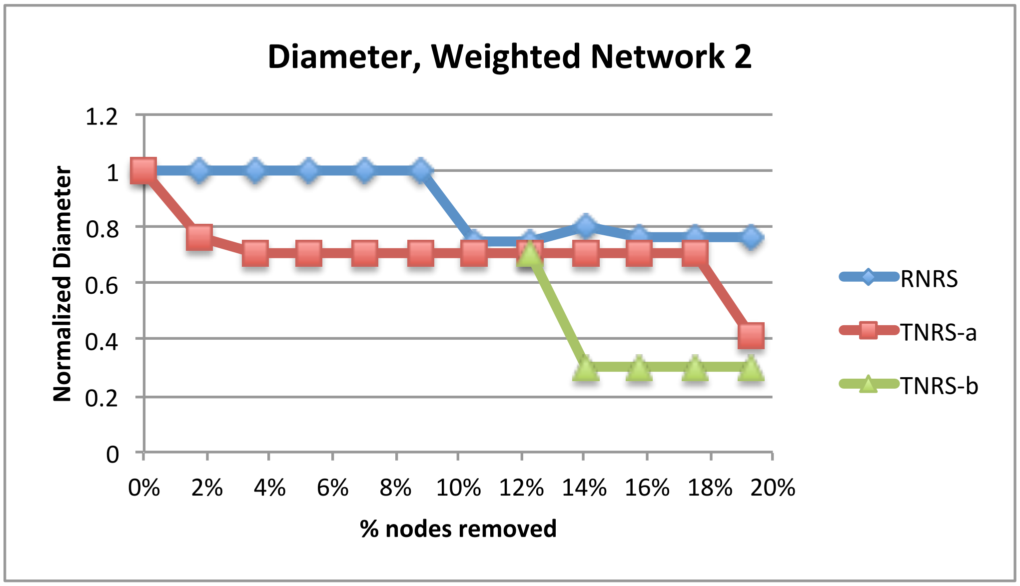


Figure 28: Diameter for Weighted Network 2

Unlike the plot for average shortest path distance of WN2 discussed earlier, some conclusions can be drawn about WN2 from the diameter plot. The diameter plot for WN2 is similar to that of the unweighted network seen in Figure 19 because the curves do not intersect. However, the RNRS and TNRS-a curves do approach each other at around 10.5% nodes removed. At that point, the values are 5% different, so that point may be called the critical point and 10.5% is the network's resilience index. Because there is no resilience index available for the average shortest path distance of WN2, 10.5% will be considered WN2's resilience index. As long as fewer than 10.5% of nodes are removed, the network is resilient to external shocks.

*Summary of Results*

Table 3 below gives a summary of the results discussed previously. The smaller value for each network is the controlling value, except in the case of WN1, where the resilience index based on diameter calculations might be misleading.

Table 3: Summary of Resilience Indices

| **Resilience Indices** | Average Shortest Path Distance | Diameter |
|---|---|---|
| Unweighted Network | 10.5% | 7% |
| WN1 | 14% | 3% * |
| WN2 | n/a ** | 10.5% |
| * *as previously discussed, possibly unreliable*<br>** *displays characteristics of scale-free network* | | |

**Conclusions**

The goal of this study was to incorporate weighting based on traffic information into a methodology for calculating a transportation network's resilience index using graph theory. Two weighting schemes were proposed: one using direct proportionality of traffic volume and the other considering the traffic volume's order of magnitude. The method was applied to a network of state and federal highways in Albemarle County, Virginia. The unweighted network's resilience index was found to be 7%. The direct proportionality method, used in WN1, led to the highest resilience index for the network, 14%. The order of magnitude method, used in WN2, also yielded a higher resilience index – 10.5% – than that of the unweighted network.

Using the direct proportionality method of WN1, the resilience index of the network increased by 100%. Twice as many nodes may be removed from the system before it is not resilient to external shock. The order of magnitude method increased the resilience index by 50%. The fact that both weighting methods increased the resilience index of the network highlights the importance of adding weights to links in analyses such as the one performed here: it offers a more complete picture of the system, and failing to include it can deflate the network's resilience index.

This study is not without its limitations. It is primarily intended to highlight the methodology used to determine a transportation network's resilience index. The use of the Albemarle County highway network is purely illustrative, and the results discussed are not meant to be used in transportation planning or maintenance efforts. In performing this analysis on the Albemarle County highway network, some simplifying assumptions were made that likely artificially deflated the resilience indices of the network. Should these be corrected, the resilience indices of the network would likely increase.

Twin bridges were modeled as a single node in this analysis. It's unlikely that both would be disabled at the same time, so if one is impassable the other could likely be used to carry traffic in both directions. The example discussed here does not consider this effect. Similarly, bridges that carry one route in the study while crossing another were modeled as a single node. This means that should that node be removed, traffic would be impeded on both the route carried and route crossed. This might be the case for a bridge collapse when both routes would be closed to traffic, but it does not consider maintenance efforts in which every care is taken to keep as many traffic lanes open as possible.

This analysis considered a total of 10 routes that run through Albemarle County. There are many smaller roads that traverse the county that were not modeled here.

This likely led to underestimations of the network's resilience because, in the event of a bridge outage on one of the routes studied, there are ways to reroute traffic around the outage using routes not studied here.

**Future Work**

There are many aspects of this study that can be expanded into opportunities for further research. In future studies, RNRS analyses for each network could be run multiple times with different node removal orders. Because the order of node removal is left up to chance in RNRS, only running the analysis once might be insufficient, especially for smaller networks. This was seen in the diameter plot for WN1, shown in Figure 25. Taking the average values of several RNRS analyses of the same network would likely lead to a more accurate resilience index for the network. The method could also be improved by the ability to partially reduce a node's functionality. In the analysis presented here, the options for a node are binary: it's either on or off. If the node's functionality could be decreased without rendering it completely inoperative, this feature could be used to simulate maintenance efforts in which care is taken to not completely impede traffic.

Further study should be done to see if the scale-free behavior observed in the average shortest path distance plot for WN2 is a feature of the weighting method or a peculiarity of the example network used here. First, the method could be applied to other types of transportation infrastructure systems, such as airport networks and railway systems, to see if they exhibit the same behavior when the order of magnitude weighting scheme is used. If they do, more in-depth analysis should be performed to determine why using the order of magnitude weighting scheme leads to scale-free behavior in transportation networks.

This method could be used to further develop the resilience index of the Albemarle County highway network. The graph would need to include not only the 10 routes studied here, but also the smaller routes that were ignored in this example. Additionally, a directed graph could be used to model traffic in each direction separately. This would eliminate the need for twin bridges to be modeled as a single node. If a bridge that has a twin is removed from the network, conditional links could be employed to reroute traffic across the other bridge, simulating how these issues are handled in the real world.

After the methodology presented here is refined, it has many real world applications and opportunities for further study. Some researchers even foresee using graph theory and resilience analysis to aid in transportation system planning and design [17].

**References**


[1] Hale, A. R.; Guldenmund, F., Goossens, L. “Auditing resilience in risk control and safety management systems” *Resilience engineering: concepts and precepts*.: Ashgate, 2006.

[2] Holling, C. S. “Resilience and Stability of Ecological Systems” Annual Review of Ecology and Systematics, Vol. 4, (1973):1-24

[3] Vugrin, E.D., Warren, D.E, Ehlen, M.A. and Camphouse, R.C. (2010) ‘A framework for assessing the resilience of infrastructures and economic systems’, Sustainable Infrastructure Systems: Simulations, Imaging, and Intelligent Engineering, Springer-Verlag, New York.

[4] MCEER. “MCEER’s Resilience Framework” <www.mceer.buffalo.edu/research /resilience/resilience_10-24-06.pdf> Accessed 3 May 2015

[5] Tierney, K. and Bruneau, M. “Conceptualizing and Measuring Resilience: A Key to Disaster Loss Reduction” TR News, No. 250 (2007):14-18

[6] Bruneau, M. and Reinhorn, A. “Exploring the Concept of Seismic Resilience for Acute Care Facilities” Earthquake Spectra. Vol. 23, No. 1 (2007):41-62

[7] O’Rourke, T.D. “Critical Infrastructure, Interdependencies, and Resilience” The Bridge Vol. 37, No. 1. (2007):23-29

[8] US. Census Bureau. “County Population Totals” <www.census.gov/popest/data /counties/totals/2014/CO-EST2014-alldata.html> Accessed 2 May 2016

[9] Silverstein Properties. “About the World Trade Center Complex” <www.wtc.com /about/overview> Accessed 22 August 2015

[10] Staff, history.com. “The Interstate Highway System.” <www.history.com/ topics/interstate-highway-system> Accessed 27 May 2016

[11] Mallett, William J., Carter, Nicole T, and Folger, Peter. “Earthquake Risk and U.S. Highway Infrastructure: Frequently Asked Questions” Congressional Research Service. June 2013

[12] Venkittaraman, Ashok, and Banerjee, Swagata. “Enhancing Resilience of Highway Bridges through Seismic Retrofit” Earthquake Engineering & Structural Dynamics, Vol. 43 (2014):1173-1191

[13] Adams, Teresa M., Toledo-Duran, Edwin, and Pavuluri, Ravi T. “Freight Corridor Performance in the Mississippi Valley Region” National Center for Freight & Infrastructure Research & Education. March 2010

[14] Balaban, A. T. “Applications of Graph Theory in Chemistry” Journal of Chemical Information and Modeling. Vol. 23, No. 3. (1985):334-343

[15] Beveridge, Andrew and Shan, Jie. “Network of Thrones” Math Horizons. Vol. 23, No. 4. (2016):18-22

[16] Attoh-Okine, Nii. “Graphs and Networks” *Resilience Engineering: Models and Analysis.* Cambridge Press, 2015.

[17] Derrible, Sybil and Kennedy, Christopher. “Applications of Graph Theory and Network Science to Transit Network Design” Transport Reviews. Vol. 31, No. 4 (2011): 495-519

[18] Giuşcă, Bogdan. “Map of Königsberg in Euler’s Time” Image, <en.wikipedia.org/wiki/Seven_Bridges_of_Königsberg> Accessed 3 June 2016

[19] Ham, Douglas B., and Lockwood, Stephen. “National Needs Assessment for Ensuring Transportation Infrastructure Security” Final Report to AASHTO Transportation Security Task Force, October 2002.

[20] Holme, P. and Kim, B. J. “Attack Vulnerability of Complex Networks” Physical Review E. Vol. 65, No. 5 (2002): 056109:1-14

[21] Guimera, R., and Amaral, L.A.N. “Modeling the world-wide airport network” European Physical Journal B, Vol. 38, No. 2 (2004): 381-385

[22] Demsar, U., Spatenkova, O. and Virrantaus, Kirsi. “Identifying Critical Locations in a Spatial Network with Graph Theory” Transactions in GIS. Vol. 12, No.1 (2008):61-82

[23] Guida, Michele, et. Al. “Topological Properties of the Italian Airport Network studied via Multiple Addendials and Graph Theory” International Journal of Mathematical models and Methods in Applied Sciences. Vol. 2, No. 2 (2008):312-316

[24] Holmgren, A. J. “Using Graph Models to Analyze the Vulnerability of Electric Power Networks” Risk Analysis. Vol. 26, No. 4. (2006): 955-969

[25] Schintler, L. A., et. Al. “Using Raster-Based GIS and Graph Theory to Analyze Complex Networks” Networks and Spatial Economics. Vol. 7, No. 4 (2007):301-313

[26] Berche, B., von Ferber, C., Holovatch, T., and Holovatch, Yu. “Resilience of Public Transport Networks Against Attacks” The European Physical Journal B. Vol. 71. No. 1 (2009): 125-137

[27] Ukkusuri, S. V. and Yushimito, W. F. “A Methodology to Assess the Criticality of Highway Transportation Networks” Journal of Transportation Security. Vol. 2, No. 1-2 (2009): 29-46

[28] Latora, V, and Marchiori, M. “Vulnerability and Protection of Infrastructure Networks” Physical Review E. Vol. 71, No. 1 (2005): 015103:1-4

[29] Leu, George, Abbass, Hussein, and Curtis, Neville. “Resilience of ground transportation networks: a case study on Melbourne” Australasian Transport Research Forum Conference (2010)

[30] Ip, W. H. and Wang, Dingwei. “Resilience Evaluation Approach of Transportation Networks” International Join Conference on Computational Sciences and Optimization. (2009):618-622

[31] Ip, W. H. and Wang, Dingwei. “Resilience and Friability of Transportation Networks: Evaluation, Analysis and Optimization” IEEE Systems Journal. Vol, 5, No. 2 (2011):189-198

[32] Dall’Asta, Luca, Barrat, Alain, Barthelemy, Marc, and Vespignani, Alessandro. “Vulnerability of Weighted Networks” Journal of Statistical Mechanics: Theory and Experiment. Vol. 2006, No. 4 (2006):PO4006:1-13

[33] Aderinlewo, Olufikayo and Attoh-Okine, Nii. “Effect of Transportation Infrastructure Network Size on its Performance during Disruptions” International Journal of Critical Infrastructures. Vol. 5, No. 3 (2009):285-298

[34] Aderinlewo, Olufikayo and Attoh-Okine, Nii. “Assessment of a Transportation Infrastructure System Using Graph Theory” Acta Technica Napocensis: Civil Engineering & Architecture. Vol. 56, No. 1 (2013):12-24

[35] Mathworks. “graph” <www.mathworks.com/help/matlab/ref/graph.html> Accessed 15 April 2016

[36] Virginia Department of Transportation. “Traffic Counts” <www.virginiadot .org/info/ct-trafficcounts.asp> Accessed 30 March 2016

[37] Albert, Reka, Jeong, Hawoong, and Barabasi, Albert-Laszlo. “Error and attack tolerance of complex networks” Nature. Vol. 406 (2000):378-382

[38] Ercal, Gunes, and Matta, John. “Resilience Notions for Scale-Free Networks” Procedia Computer Science. Vol. 20 (2013):510-515

## Appendix A: Bridge Node Information

| Node # | Road Carried | Structure Number | Year Built | Lanes Carried | Bridge Kind | Bridge Type |
|---|---|---|---|---|---|---|
| 1 | VA-6 | 415 | 1932 | 2 | concrete | deck arch |
| 2 | VA-6 | 408 | 1935 | 2 | concrete | tee beam |
| 3 | VA-6 | 407 | 1935 | 2 | concrete | tee beam |
| 4 | VA-20 | 443 | 1970 | 2 | prestressed concrete | stringer/multi-beam or girder |
| 5 | VA-20 | 420 | 1932 | 2 | concrete | slab |
| 6 | VA-20 | 27152 | 2004 | 2 | steel continuous | stringer/multi-beam or girder |
| 7 | VA-20 | 23360 | 1992 | 2 | prestressed concrete | slab |
| 8 | VA-20 | 447 | 1968 | 2 | steel | stringer/multi-beam or girder |
| 9 | VA-22 | 454 | 1932 | 2 | concrete | slab |
| 10 | VA-22 | 452 | 1932 | 2 | concrete | slab |
| 11 | VA-22 | 451 | 1932 | 2 | concrete | slab |
| 12 | VA-22 | 449 | 1923 | 2 | concrete | slab |
| 13 | VA-22 | 448 | 1935 | 2 | prestressed concrete | box beam or girders-multiple |
| 14 | US-29 | 481 | 1965 | 2 | steel | stringer/multi-beam or girder |
| 15 | US-29 | 25821 | 1897 | 4 | steel continuous | stringer/multi-beam or girder |
| 16 | US-29 | unknown | 2012 | 6 | steel | stringer/multi-beam or girder |
| 17 | US-29 | 475 | 1977 | 4 | steel | stringer/multi-beam or girder |
| 18 | US-29 | 621 | 1961 | 5 | steel | stringer/multi-beam or girder |
| 19 | US-29 | 484 | 1970 | 4 | steel | stringer/multi-beam or girder |
| 20 | US-29 | 552 | 1970 | 3 | prestressed concrete | stringer/multi-beam or girder |
| 21 | US-29 | 461 | 1976 | 2 | steel | stringer/multi-beam or girder |
| 22 | US-29 | 25120 | 1997 | 2 | concrete | stringer/multi-beam or girder |
| 23 | VA-53 | 27374 | 2005 | 2 | steel | stringer/multi-beam or girder |
| 24 | I-64 | 517 | 1974 | 2 | steel | stringer/multi-beam or girder |
| 25 | I-64 | 507 | 1974 | 2 | steel | stringer/multi-beam or girder |
| 26 | I-64 | 759 | 1972 | 2 | steel | stringer/multi-beam or girder |
| 27 | I-64 | 546 | 1969 | 2 | prestressed concrete | stringer/multi-beam or girder |
| 28 | I-64 | 550 | 1969 | 2 | steel continuous | stringer/multi-beam or girder |
| 29 | I-64 | 696 | 1969 | 2 | prestressed concrete | stringer/multi-beam or girder |
| 30 | I-64 | 554 | 1969 | 2 | steel continuous | stringer/multi-beam or girder |
| 31 | I-64 | 556 | 1969 | 2 | prestressed concrete | stringer/multi-beam or girder |
| 32 | I-64 | 572 | 1970 | 2 | steel | stringer/multi-beam or girder |
| 33 | I-64 | 562 | 1970 | 3 | steel | stringer/multi-beam or girder |

**Appendix A Continued**

| Node # | Road Carried | Structure Number | Year Built | Lanes Carried | Bridge Kind | Bridge Type |
|---|---|---|---|---|---|---|
| 34 | I-64 | 564 | 1970 | 2 | steel | stringer/multi-beam or girder |
| 35 | | 568 | 1970 | 2 | prestressed concrete | stringer/multi-beam or girder |
| 36 | | 682 | 1969 | 4 | steel | stringer/multi-beam or girder |
| 37 | | 522 | 1969 | 3 | prestressed concrete | stringer/multi-beam or girder |
| 38 | | 526 | 1969 | 3 | steel | stringer/multi-beam or girder |
| 39 | | 534 | 1969 | 2 | steel continuous | girder and floorbean system |
| 40 | | 530 | 1969 | 2 | steel continuous | frame |
| 41 | | 540 | 1969 | 2 | concrete | tee beam |
| 42 | | 536 | 1969 | 2 | steel | stringer/multi-beam or girder |
| 43 | | 657 | 1969 | 2 | steel | stringer/multi-beam or girder |
| 44 | | 544 | 1969 | 2 | steel continuous | stringer/multi-beam or girder |
| 45 | VA-231 | 581 | 1939 | 2 | concrete | slab |
| 46 | VA-240 | 589 | 1921 | 2 | concrete | tee beam |
| 47 | | 591 | 1921 | 2 | prestressed concrete | box beam or girders-multiple |
| 48 | US-250 | 602 | 1945 | 2 | prestressed concrete | box beam or girders-multiple |
| 49 | | 601 | 1945 | 2 | steel | stringer/multi-beam or girder |
| 50 | | 598 | 1942 | 2 | steel | stringer/multi-beam or girder |
| 51 | | 596 | 1936 | 2 | concrete | frame |
| 52 | | 610 | 1932 | 3 | concrete | slab |
| 53 | | unknown | 2006 | 5 | steel | stringer/multi-beam or girder |
| 54 | | unknown | 2013 | 4 | steel | stringer/multi-beam or girder |
| 55 | | 23447 | 1992 | 7 | steel continuous | stringer/multi-beam or girder |
| 56 | | 595 | 1939 | 2 | prestressed concrete | box beam or girders-multiple |
| 57 | | 607 | 1932 | 3 | concrete | slab |

## Appendix B: Intersection Node Information

| Node # | Feature 1 | Feature 2 |
|---|---|---|
| 58 | I-64 | Nelson County Line |
| 59 | US-250 | Nelson County Line |
| 60 | VA-151 | Nelson County Line |
| 61 | US-29 | Nelson County Line |
| 62 | VA-6 | Nelson County Line |
| 63 | VA-53 | Fluvanna County Line |
| 64 | US-250 | Fluvanna County Line |
| 65 | I-64 | Fluvanna County Line |
| 66 | VA-22 | Louisa County Line |
| 67 | VA-231 | Louisa County Line |
| 68 | VA-20 | Orange County Line |
| 69 | US-29 | Greene County Line |
| 70 | US-250 | VA-151 |
| 71 | US-250 | VA-240 (south of Crozet) |
| 72 | US-250 | VA-240 (east of Crozet) |
| 73 | VA-6 | VA-20 |
| 74 | VA-22 | VA-231 |
| 75 | US-29 BUS | US-250 BUS |
| 76 | VA-20 | US-250 BUS |
| 77 | VA-20 | VA-53 |
| 78 | US-250 BUS | US-250 BYP |
| 79 | US-250 BYP | VA-20 |
| 80 | US-250 | VA-22 |

## Appendix C: Link Information

| link # | route | start node | end node | distance (miles) | AADT | WN1 Weight | WN2 Weight |
|---|---|---|---|---|---|---|---|
| 1 | VA-6 | 62 | 1 | 2.24 | 1144 | 1.96E+00 | 7.31E-01 |
| 2 | | 1 | 2 | 9.38 | | 8.20E+00 | 3.07E+00 |
| 3 | | 2 | 3 | 0.31 | | 2.72E-01 | 1.02E-01 |
| 4 | | 3 | 73 | 0.68 | | 5.97E-01 | 2.23E-01 |
| 5 | VA-20 | 68 | 79 | 13.55 | 13096 | 1.03E+00 | 3.29E+00 |
| 6 | | 76 | 4 | 1.49 | 12795 | 1.17E-01 | 3.63E-01 |
| 7 | | 4 | 38 | 0.25 | | 1.94E-02 | 6.05E-02 |
| 8 | | 38 | 77 | 0.50 | 22000 | 2.26E-02 | 1.14E-01 |
| 9 | | 77 | 5 | 1.30 | 7059 | 1.85E-01 | 3.39E-01 |
| 10 | | 5 | 6 | 6.84 | | 9.68E-01 | 1.78E+00 |
| 11 | | 6 | 7 | 1.68 | | 2.38E-01 | 4.36E-01 |
| 12 | | 7 | 73 | 7.02 | | 9.95E-01 | 1.82E+00 |
| 13 | | 73 | 8 | 0.87 | | 1.23E-01 | 2.26E-01 |
| 14 | VA-22 | 80 | 9 | 3.79 | 7728 | 4.90E-01 | 9.75E-01 |
| 15 | | 9 | 74 | 1.30 | | 1.69E-01 | 3.36E-01 |
| 16 | | 74 | 10 | 0.93 | 1800 | 5.18E-01 | 2.86E-01 |
| 17 | | 10 | 11 | 0.12 | | 6.90E-02 | 3.82E-02 |
| 18 | | 11 | 12 | 1.68 | | 9.32E-01 | 5.15E-01 |
| 19 | | 12 | 13 | 0.25 | | 1.38E-01 | 7.64E-02 |
| 20 | | 13 | 66 | 0.68 | | 3.80E-01 | 2.10E-01 |
| 21 | US-29 | 69 | 14 | 3.17 | 41995 | 7.55E-02 | 6.85E-01 |
| 22 | | 14 | 15 | 4.10 | | 9.77E-02 | 8.87E-01 |
| 23 | | 15 | 16 | 3.54 | | 8.43E-02 | 7.66E-01 |
| 24 | US-29 bypass | 16 | 17 | 0.50 | 37000 | 1.34E-02 | 1.09E-01 |
| 25 | | 17 | 18 | 1.37 | 47000 | 2.91E-02 | 2.93E-01 |
| 26 | | 18 | 19 | 1.55 | 45000 | 3.45E-02 | 3.34E-01 |
| 27 | US-29 business | 16 | 75 | 1.37 | 24714 | 5.53E-02 | 3.11E-01 |
| 28 | | 75 | 19 | 1.93 | 11975 | 1.61E-01 | 4.72E-01 |
| 29 | US-29 | 19 | 20 | 0.62 | 51000 | 1.22E-02 | 1.32E-01 |
| 30 | | 20 | 21 | 6.03 | 14484 | 4.16E-01 | 1.45E+00 |
| 31 | | 21 | 22 | 5.78 | | 3.99E-01 | 1.39E+00 |
| 32 | | 22 | 61 | 4.66 | | 3.22E-01 | 1.12E+00 |
| 33 | VA-53 | 77 | 23 | 7.77 | 7576 | 1.03E+00 | 2.00E+00 |
| 34 | | 23 | 63 | 1.80 | | 2.38E-01 | 4.64E-01 |
| 35 | I-64 | 58 | 24 | 1.93 | 33000 | 5.84E-02 | 4.26E-01 |
| 36 | | 24 | 25 | 0.75 | | 2.26E-02 | 1.65E-01 |
| 37 | | 25 | 26 | 2.05 | | 6.21E-02 | 4.54E-01 |
| 38 | | 26 | 27 | 1.43 | | 4.33E-02 | 3.16E-01 |
| 39 | | 27 | 28 | 0.87 | 38000 | 2.29E-02 | 1.90E-01 |
| 40 | | 28 | 29 | 0.62 | | 1.64E-02 | 1.36E-01 |
| 41 | | 29 | 30 | 1.74 | | 4.58E-02 | 3.80E-01 |
| 42 | | 30 | 31 | 0.62 | | 1.64E-02 | 1.36E-01 |
| 43 | | 31 | 32 | 3.23 | | 8.50E-02 | 7.06E-01 |

**Appendix C Continued**

| link # | route | start node | end node | distance (miles) | AADT | WN1 Weight | WN2 Weight |
|---|---|---|---|---|---|---|---|
| 44 | I-64 | 32 | 20 | 3.79 | 39000 | 9.72E-02 | 8.26E-01 |
| 45 | | 20 | 33 | 0.19 | 48000 | 3.88E-03 | 3.98E-02 |
| 46 | | 33 | 34 | 0.62 | | 1.29E-02 | 1.33E-01 |
| 47 | | 34 | 35 | 0.50 | | 1.04E-02 | 1.06E-01 |
| 48 | | 35 | 36 | 0.25 | | 5.18E-03 | 5.31E-02 |
| 49 | | 36 | 37 | 0.19 | 37000 | 5.04E-03 | 4.08E-02 |
| 50 | | 37 | 38 | 1.55 | | 4.20E-02 | 3.40E-01 |
| 51 | | 38 | 39 | 1.55 | | 4.20E-02 | 3.40E-01 |
| 52 | | 39 | 40 | 1.12 | | 3.02E-02 | 2.45E-01 |
| 53 | | 40 | 41 | 1.68 | 37169 | 4.51E-02 | 3.67E-01 |
| 54 | | 41 | 42 | 0.50 | | 1.34E-02 | 1.09E-01 |
| 55 | | 42 | 43 | 3.23 | | 8.69E-02 | 7.07E-01 |
| 56 | | 43 | 44 | 0.93 | | 2.51E-02 | 2.04E-01 |
| 57 | | 44 | 65 | 0.25 | | 6.69E-03 | 5.44E-02 |
| 58 | VA-151 | 60 | 70 | 1.12 | 9700 | 1.15E-01 | 2.81E-01 |
| 59 | VA-231 | 74 | 45 | 6.84 | 4900 | 1.39E+00 | 1.85E+00 |
| 60 | | 45 | 67 | 1.24 | | 2.54E-01 | 3.37E-01 |
| 61 | VA-240 | 71 | 46 | 0.62 | 5883 | 1.06E-01 | 1.65E-01 |
| 62 | | 46 | 47 | 3.36 | | 5.70E-01 | 8.90E-01 |
| 63 | | 47 | 72 | 0.19 | | 3.17E-02 | 4.95E-02 |
| 64 | US-250 | 59 | 70 | 1.74 | 6200 | 2.81E-01 | 4.59E-01 |
| 65 | | 70 | 48 | 0.50 | 6235 | 7.97E-02 | 1.31E-01 |
| 66 | | 48 | 49 | 0.62 | | 9.97E-02 | 1.64E-01 |
| 67 | | 49 | 27 | 3.67 | | 5.88E-01 | 9.66E-01 |
| 68 | | 27 | 71 | 1.62 | 11000 | 1.47E-01 | 4.00E-01 |
| 69 | | 71 | 72 | 2.98 | 9100 | 3.28E-01 | 7.53E-01 |
| 70 | | 72 | 50 | 0.06 | 12538 | 4.96E-03 | 1.52E-02 |
| 71 | | 50 | 51 | 2.98 | | 2.38E-01 | 7.28E-01 |
| 72 | | 51 | 52 | 0.81 | | 6.44E-02 | 1.97E-01 |
| 73 | | 52 | 18 | 3.17 | | 2.53E-01 | 7.73E-01 |
| 74 | US-250 business | 18 | 75 | 1.18 | 12000 | 9.84E-02 | 2.89E-01 |
| 75 | | 75 | 76 | 2.17 | 22502 | 9.66E-02 | 5.00E-01 |
| 76 | | 76 | 78 | 0.87 | 13555 | 6.42E-02 | 2.11E-01 |
| 77 | US-250 bypass | 16 | 53 | 1.43 | 31805 | 4.49E-02 | 3.17E-01 |
| 78 | | 53 | 54 | 0.31 | 32474 | 9.57E-03 | 6.89E-02 |
| 79 | | 54 | 78 | 1.06 | | 3.25E-02 | 2.34E-01 |
| 80 | US-250 | 78 | 55 | 0.06 | | 1.91E-03 | 1.38E-02 |
| 81 | | 55 | 79 | 0.19 | 30458 | 6.12E-03 | 4.16E-02 |
| 82 | | 79 | 40 | 1.74 | | 5.71E-02 | 3.88E-01 |
| 83 | | 40 | 80 | 2.05 | 22000 | 9.32E-02 | 4.72E-01 |
| 84 | | 80 | 56 | 0.12 | 5200 | 2.39E-02 | 3.34E-02 |
| 85 | | 56 | 57 | 2.67 | | 5.14E-01 | 7.19E-01 |
| 86 | | 57 | 64 | 1.62 | | 3.11E-01 | 4.35E-01 |

## Appendix D: Link Density and Average Node Degree Plots for Weighted Networks

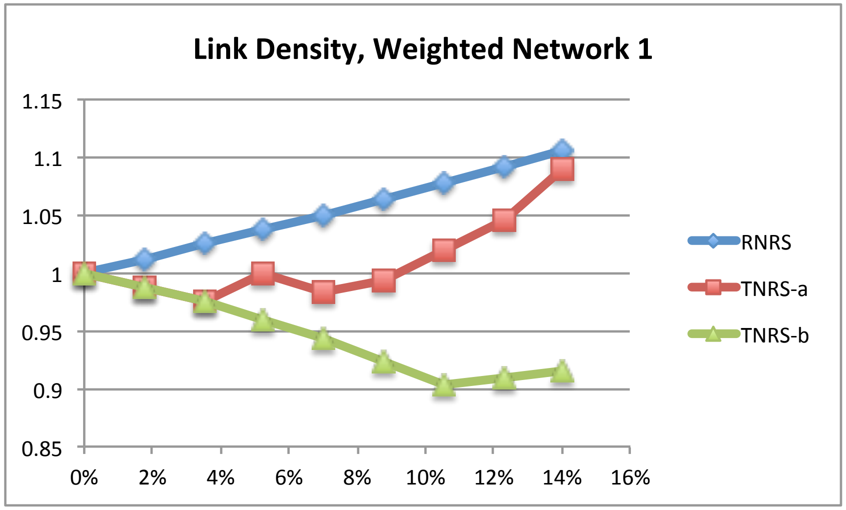


Figure D1: Link Density for Weighted Network 1

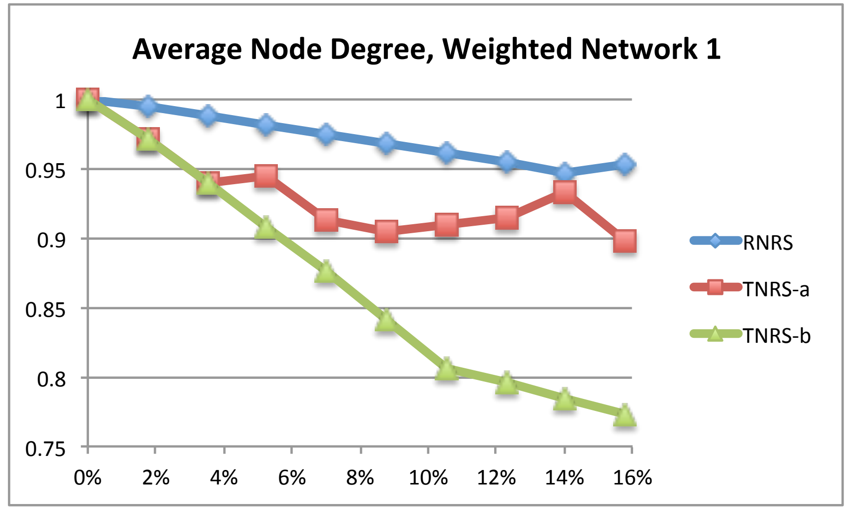


Figure D2: Average Node Degree for Weighted Network 1

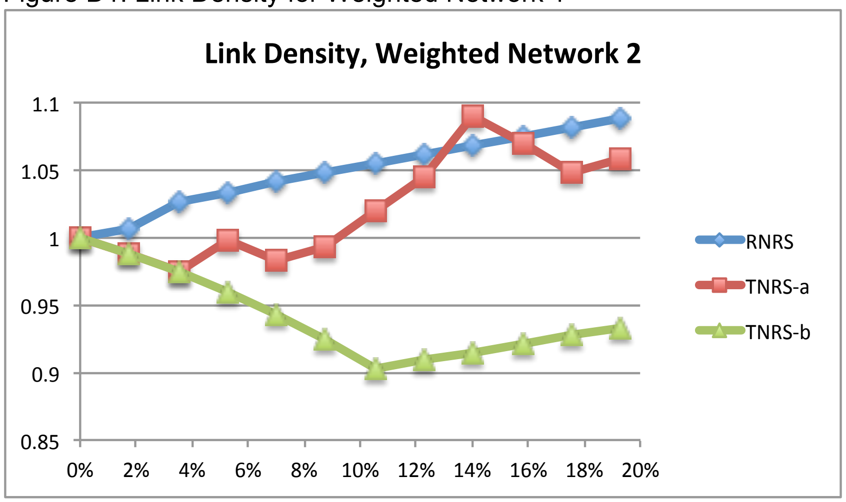


Figure D3: Link Density for Weighted Network 2

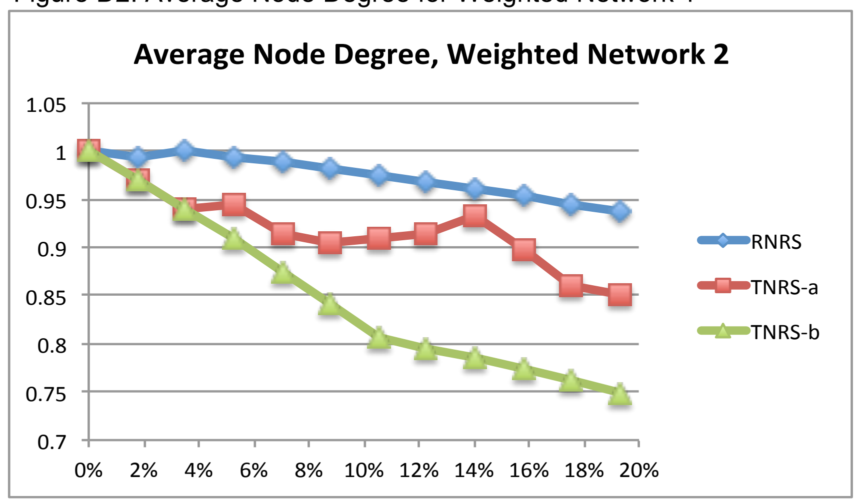


Figure D4: Average Node Degree for Weighted Network 2